Contents lists available at ScienceDirect

Quaternary Science Reviews

journal homepage: www.elsevier.com/locate/quascirev

# The Late Pleistocene and Holocene chronocultural and anthracological open-air sequence from Mukila (DRC)

Katharina V.M. Jungnickel [a,*], Dirk Seidensticker [b], Wannes Hubau [c,e], Florias Mees [f], Els Cornelissen [d], Koen Bostoen [g]

[a] Institute of Archaeological Sciences, Goethe University Frankfurt, Germany
[b] Department of Archaeology, Ghent University, Belgium
[c] Service of Wood Biology, Royal Museum for Central Africa, Tervuren, Belgium
[d] Department of Cultural Anthropology and History, Royal Museum for Central Africa, Tervuren, Belgium
[e] Department of Environment, Laboratory of Wood Technology (Woodlab), Ghent University, Belgium
[f] Service of Surface Environments and Collection Management, Royal Museum for Central Africa, Tervuren, Belgium
[g] Department of Languages and Cultures, Ghent University, Belgium

ARTICLE INFO

Handling editor: Giovanni Zanchetta

ABSTRACT

Late Pleistocene and Early Holocene open-air archaeological sites have been assumed to be disturbed throughout Central Africa because key sites located on the Kalahari Sand Belt and excavated in the 1970s documented substantial artefact displacement. As a result, only cave sites have long been seen as suitable for presenting reliable vertical chrono-cultural sequences, and minimal effort was made to investigate open-air sites in Central Africa. This paper presents a multi-disciplinary approach combining archaeological, anthracological, and sediment granulometry data to test the vertical integrity of detailed excavations at the open-air site Mukila (DRC). Refitting analysis shows only minor vertical displacement of lithics (6306 artefacts), pottery (1095 sherds) and charcoal (447 fragments), along with a uniform soil particle size distribution throughout the profile. A chronology of 16 radiocarbon dates confirms a continuous age-depth relationship at the site. These data reveal a mostly intact stratigraphy spanning the last 40,000 years. We thus demonstrate that sites along the northern edges of the Kalahari Sand Belt do not per se show vertical disturbance of charcoal and artefact distribution despite uniform grain size distribution. We conclude that a multi-disciplinary approach is mandatory for studying the integrity of archaeological sequences from Central African open-air sites.

## 1. Introduction

Archaeological knowledge of the Late Pleistocene and Early Holocene in Central Africa (older than circa 2000 BCE) relies on very few sites. Most well-studied Stone Age sites are located at the northern fringes of the rainforest (Cornelissen, 1996, 2003; Lavachery, 1996, 1997, 2001; Lupo et al., 2021) and from the Congo Basin, lithics are solely known from surface collections (Preuβ and Fiedler, 1984; Fiedler and Preuβ, 1985). On the western Batéké Plateau, at the southern margin of the rainforest, some archaeological research was conducted (de Bayle des Hermens and Lanfranchi, 1978; Dupré and Pinçon, 1997; Kouyoumontzakis et al., 1985; Lanfranchi and Pinçon, 1988; Pinçon, 1984, 1990, 1991a, 1991b), while the eastern part saw very little engagement (van Moorsel, 1970; Cornelissen and Livingstone Smith, 2015; Seidensticker et al., 2018). Isolated finds are reported near Bandundu (Creppe, 1935; Vanderyst, 1950, Fig. 1A). Extensive surveys and excavations (1950–1952) by Maurice Bequaert accrued a handful of sites, most notably Dinga Kiitu (formerly Ndinga St. Pierre) and Mukila (Fig. 1A) (Bequaert, 1953, 1955, 1956a, 1956b, 1956c).

The principal, recurrently cited, reference sequence for the lithic industries of the Late Pleistocene and Holocene in that region is Gombe (Kinshasa, DRC; Fig. 1; Clark, 1971; Cahen, 1976; Cahen et al., 1983; de Maret, 1990; de Maret and Stainier, 1999). An extensive refitting program and chronometric dates revealed discrepancies in the site's integrity (Cahen, 1976, 1978). Refits of strictly contemporaneous lithic artefacts crossed the established sequence of Holocene (Ndolian) and Pleistocene (Djokocian/Kalinian) industries. The conclusions of these studies indicate severe vertical disturbances of archaeological materials.

* Corresponding author.
E-mail address: Katharina.Jungnickel@ugent.be (K.V.M. Jungnickel).

https://doi.org/10.1016/j.quascirev.2024.108752
Received 29 November 2023; Received in revised form 28 April 2024; Accepted 1 June 2024

Consequently, it was derived that no direct relationship was to be established between a radiocarbon-dated charcoal sample and artefacts at similar depths (Cahen et al., 1983). Cahen and Moeyersons (1977) deduce that their observations "strongly suggest that this process of redistribution has a general and systematic character in the entire area covered by Kalahari-type sands in Central Africa" (cf. Fig. 1A), thereby discouraging any investigations into open-air sites. This generalisation led to stagnation and inevitably perpetuation and recycling of the same state of knowledge (Taylor, 2011, 2016, 2022).

Contrary to this, one already existing example of good site integrity, showing no vertical severe post-depositional disturbances, was observed at Batéké (Plateau Teke) (Fig. 1A; Cahen and Mortelmans, 1973). Archaeologically sterile layers of sands clearly separated Tshitolian lithic artefacts from an ancient soil surface where a Lupemban core was found. Consequently, the question arises whether the predominant paradigm set by Cahen and Moeyersons (1977) holds true. This question is substantial as open-air sites are more abundant than caves and could potentially provide a wealth of archaeological information. In this paper, we therefore focus on the site of Mukila, which yielded an abundance of artefacts and charcoal and was excavated to a depth of 6 m, allowing a thorough investigation of site integrity.

The site of Mukila was first excavated by Maurice Bequaert in 1952 and is notable among the collections of the Royal Museum for Central Africa (RMCA, Tervuren, Belgium) because of the co-occurrence of lithics and pottery. The uniqueness of the 1952 collection and easy accessibility of the site initiated a 2018 re-investigation (Seidensticker et al., 2018), whose initial objective was to gain better resolution of the transition from lithic industries to the first introduction of pottery south of the equatorial rainforest. Insight into the lithic industries defining the communities living in Central Africa prior to the introduction of pottery is critical to comprehending any putative interactions between communities of different subsistence. A crucial precondition regarding the interpretative value of the results from Mukila is a rigorous assessment of the integrity of the uncovered sequence, especially considering the disturbances observed at Gombe (Cahen, 1976, 1978).

Hence, the objective of this paper is to test the site integrity at Mukila by following a multi-disciplinary approach and analysing its lithics, pottery, and botanical remains. With Bequaert's field documentation showing no lithological units and our 2018 excavation equally yielding no discernible stratigraphic units, we developed a spatially informed

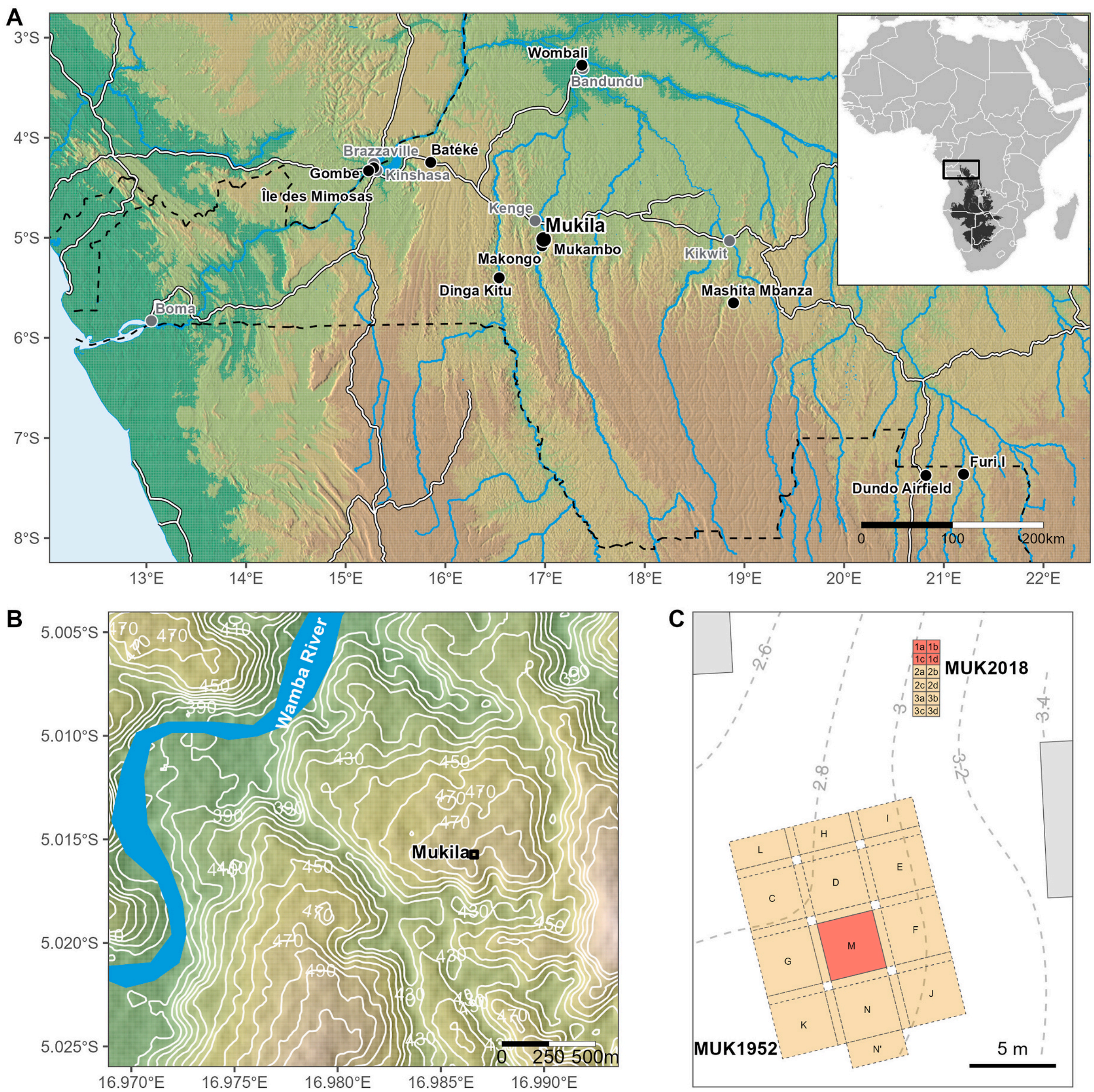


**Fig. 1.** Map of Mukila in the broader region (**A**), the hilltop topography (**B**) and the location of *Gite II B* (*MUK1952*) and *MUK2018* (**C**) in reference to school buildings (grey). Red quadrants (**C**) were used for the refit analysis. The extent of the Kalahari group in black (insert in **A**) after Haddon and McCarthy, 2005: 318.

intra-site framework corresponding to a post-excavation stratigraphy (Discamps et al., 2023), mainly relying on the species distribution of botanical remains to create meaningful zoning within the stratigraphy. We combine the artefacts and documentation from the collection of 1952 (Bequaert, 1956b, 1956c) with a new excavation conducted in 2018 (Seidensticker et al., 2018), due to the older excavation providing a larger lithic artefact inventory and the 2018 excavation being better documented.

## 2. Regional setting

The village of Mukila is located some 250 km east of Kinshasa (Figs. 1A) and 25 km south of the provincial capital Kenge. The site 'Mukila École' is situated on a hilltop (480 m ASL), roughly 120 m above the Wamba River (360 m ASL). The hill has a steep southern and eastern slope and a gentler western slope towards the river (Fig. 1B). This location is similar to other sites in the region, like the hilltop of Mukambo, which was also investigated by Bequaert (Bequaert, 1955, 1956a, 1956b; Miller, 2001). These hills are remnants of the Batéké Plateau that extend to the south and west of the Mukila area (Nieto--Quintano et al., 2018), where a series of north-flowing rivers cross it. The Batéké Plateau is a northern extension of the vast region covered by Kalahari Group deposits (Fig. 1A), which reaches as far south as the Orange River in South Africa (Thomas and Shaw, 1991: 6 Fig. 1.2; 8; Haddon and McCarthy, 2005). In this northern area, the *Série des Grès Polymorphes*, with assumed Paleogene age, is regarded as the equivalent of the Kalahari Group (Cahen and Lepersonne, 1952). This formation is overlain by *Série des Sables Ocre* deposits, attributed to the Neogene (ibid.) and interpreted as having formed by low-energy fluviatile sedimentation in an arid environment (De Ploey et al., 1968).

The Mukila hill has been mapped as having deposits of the *Série des Grès Polymorphes* at its summit, lacking the overlying *Série des Sables Ocre* deposits that do occur on most of the neighbouring hills, as well as on the plateau from which they are derived (unpublished geological map, sheet Popokabaka S6/16, scale 1/200.000; RMCA archives). Around the hill of Mukila, the Cretaceous deposits that underlie the sandstones of the *Série des Grès Polymorphes* are exposed by erosion. Environmentally, the area is situated on the southern margins of the equatorial rainforest and shows a mosaic-like pattern of dense vegetation within the valleys of the main rivers. Mukila lies within a tropical savannah climate (Köppen-Geiger: Aw; Peel et al., 2007), and the modern vegetation is that of mosaic forest/savanna neighboured by closed evergreen lowland forest in the river valley (Mayaux et al., 2003).

## 3. Materials and methods

### *3.1. New excavation in 2018*

The trench MUK 2018/1000/30 (hereafter *MUK2018*) covered a 1.5 on 4.5 m surface and was excavated to 3.6 m below the surface. The trench (Fig. 1C) was subdivided into three squares (1–3), each subdivided into four 75 × 75 cm quadrants (a-d) and excavated in spits of 20 cm depth, with a total of 126 units. For safety and practicability, for every three spits (60 cm), two quadrants at the southern end of the excavated area were left standing and used as steps (Fig. S1). The maximum depth of 3.6 m was only reached at the northern profile in quadrants 1 a/b and extended by coring another 3 m to 6.6 m below the surface (Seidensticker et al., 2018, 26–27). All sediments were dry-sieved for small finds through a mesh size of 4 mm, and all paleoenvironmental remains, such as charcoal fragments, were systematically sampled.

### *3.2. Re-examination of the 1952 collection*

In 1952, Maurice Bequaert excavated multiple sites in and around the town of Mukila (Bequaert, 1956b, 1956c). The most extensive excavation is at the local school ('Mukila École'), where an eleven-by-thirteen-metre large trench (*Gite II B*) was excavated up to nearly 7 m below the surface. The trench was subdivided into thirteen alphabetically labelled units (Fig. 1C; Fig. S2; S3). While depths of finds were recorded in the field and the excavation proceeded in steps, there are no records of controlled spits. All documentation from Maurice Bequaert's fieldwork is archived at the RMCA and consists of notebooks and loose pages containing geodetic measurements, sketches, and photographs (Fig. S2; S3). The photographs allowed the exact position of the trench to be relocated at the site 'Mukila École'. With the help of those images and through interviews with local inhabitants, we could accurately determine the angle from which the photos had been taken and consequently retrace the location of trench 'Gite II B' (hereafter *MUK1952*). The trench outline and the school buildings are visible in the photographs, and large printouts referenced the position on-site. A new panorama (Fig. S2) helped digitally reference the old and new photos. Measuring the distance between the buildings, we located a still-existing, prominent palm tree visible in the images from 70 years ago. On-site, those points of reference helped triangulate a position for a new trench close to the palm tree near Bequaert's trench without cutting into the area of his infill. We reproduced the geodetic survey conducted by Bequaert in 1952 and referenced it to our geodetic survey from 2018. By doing so, we could adequately georeference the *MUK1952* excavation (Fig. 1C).

Besides the documentation, the RMCA collection contains nearly 3000 objects from the 1952 Mukila École excavation, mainly lithics, about 500 ceramic sherds, and eight charcoal samples. The ceramics and lithics from the collection were depth-referred based on Bequaert's documentation and inscriptions on the objects. Each excavation unit has a unique RMCA inventory number, resulting in 767 entities containing at least one object. While the largest entity comprises 309 objects (InvNo. 62389), about 70 % of all units only include one object. All objects had been labelled with a museum inventory number, and larger pieces often retain the field labelling of the site's name, trench, square, excavation date and depth. Except for the inventory number, the handwriting on the pieces matches the one in Bequaert's notebooks.

While the depth of finds was recorded in two modes in the field, either within or without parentheses, we could reconstruct the depth below the surface by cross-referencing multiple objects with both types of notations (Fig. S4) and Bequaert's field notes. This corresponds to 3% of all inventoried items, and in each case, the value in parentheses is always higher than that without parentheses. The values differ by zero to 9 cm in four cases, whereas another four show a 47 or 52 cm difference between the depth values in parentheses and those without. A reconstruction of Bequaert's old excavation reference point based on georeferencing his geodetic measurements showed that Bequaert consistently used a single point northeast of this trench and between both school buildings as a station for his theodolite (Fig. S2). The depth values of his multi-day geodetic survey match those noted in an overview map of the trench (Fig. S3), indicating that the station was coherently used to record depths. On our topographic mapping of the site from 2018, the location of the datum point from 1952 is around 50 cm higher than the reconstructed location of square *M*, thus further corroborating the field notes. As the depth values in parentheses are systematically higher than those without parentheses, in all cases where both notations were recorded, we consider all depths in parentheses (71% of all inventory items) resulting from measurements using the datum, while those without parentheses (26% of all inventory units) correspond to the surface at the time. Thus, in cases where only depth below the datum is recorded, values are deduced by 42 cm, referring to a small record card showing a generalised profile of the northern wall of *M* (Fig. S5). The depth recorded by Bequaert was allotted to the 20 cm spits of *MUK2018* to compare the inventories from both excavations.

While the extent of the trench *MUK1952* was barely visible on the modern surface (Fig. S2), systematic levelling revealed that square *M* of *MUK1952* lies, on average, about 10 cm lower than the surface at square

1 in *MUK2018*. Interpolation of our levelling revealed that the datum from 1952 was located around 30 cm higher than the surface at *MUK2018*. The area of *MUK1952* saw substantial post-excavation earthworks, especially the excavation of latrines in the old backfill (Fig. S2). Thus, the precise difference in surface levels between *MUK1952* and *MUK2018* cannot be reconstructed. Consequently, all depths below the surface reference the respective excavation, keeping in mind that the surface of *MUK1952* has been slightly lower than that of *MUK2018*. Despite the historical nature of the 1952 fieldwork, the detailed examination of the available collection and documentation revealed that this type of data can be reconstructed and made accessible.

### 3.3. Charcoal analysis

Paleoenvironmental remains from the 2018 excavation were carefully washed on a sieve with a mesh size of 1 mm, oven-dried at 40 °C for 48 h and stored in plastic boxes per square and per spit. Fruit-derived charcoal remains were separated from wood-derived charcoal fragments using a stereomicroscope. Endocarp and wood-derived charcoal collections were weighed on an analytical balance (Sartorius) with 0.1 mg precision for each square and spit. As the total sieved volume for each square and each spit is known, fruit- and wood-derived charcoal abundance was expressed as mg charcoal per litre sediment (mg $l^{-1}$). Fruit-derived charcoal fragments were further examined using a stereomicroscope and compared to a reference collection of fruits available at the RMCA. As in many archaeological excavations in Central Africa (Oas et al., 2015), most fruit remains were identified as oil palm endocarp (*Elaeis guineensis*) and some as endocarp of *Canarium schweinfurthii*. At least twenty wood-derived charcoal fragments from each spit were randomly selected for wood-anatomical examination using standard methods (Hubau et al., 2012). Each charcoal fragment was broken carefully by hand to expose fresh and clean observation planes of the three primary wood-anatomical surfaces (transversal, radial and tangential) (Fig. S6). Each observation plane was then mounted on a coded microscope glass using Plaxtin plastilene. The surfaces were inspected using an Olympus BX60 reflected light microscope with 100×, 200× and 500× magnification. During the microscopic inspection, charcoal fragments were grouped into charcoal types, of which each type generally represents a group of lookalike tree species mostly belonging to a single genus (Hubau et al., 2015).

During microscopic inspection, charcoal types were described by applying the numbered anatomical features defined by the International Association of Wood Anatomists (IAWA Committee, 1989) and used for the online InsideWood database (Hubau et al., 2012; IAWA Committee, 1989; Inside Wood Database, 2016; Wheeler, 2011). This produces a string of numbered features for each charcoal type. Finally, for each charcoal type, the string of anatomical features was used for preliminary identification on the InsideWood database, which returns a group of possible species for each charcoal type. This preliminary identification was used to confirm that each charcoal type is unique, representing a different (group of) species. Each distinctly different charcoal type received a number, starting with the first type found in the uppermost spit. To illustrate that each charcoal type has a different set of wood anatomical features, anatomical descriptions of the five most abundant charcoal types were refined to identify the type down to genus level using InsideWood. Scanning Electron Microscope (SEM) images of these charcoal types are shown in Fig. S6. Full anatomical descriptions using IAWA features are presented in Tab. S1 (IAWA Committee, 1989). Strings of numbered anatomical features used on InsideWood for genus identification are given in Tab. S2.

The charcoal-type abundance data was used to separate statistically different spits using constrained hierarchical clustering with the chclust command of the Rioja package in R (Juggins, 2012). Based on the Mantel statistic, we defined the optimum number of depth zones (Borcard et al., 2011). Charcoal types were clustered similarly, and we used both chclust objects in the tabasco function to produce an ordered community table (Oksanen et al., 2018).

### 3.4. Radiocarbon dating

Clustering analysis of the spits resulted in seven different depth zones. For each zone, one charcoal fragment was selected for radiocarbon dating. We selected a fragment from charcoal types with clear anatomy and no fragments in an adjacent zone (just above or below the zone of interest). We selected oil palm endocarps for radiocarbon dating in the first two zones. Four zones received two or three radiocarbon dates. In total, 13 fragments were selected for radiocarbon dating in *MUK2018* (Table 1).

The museum collections also contained eight wood-derived charcoal samples collected by M. Bequaert in 1952. Two samples had proper contextualisation because the depth was noted in parentheses on a piece of paper adjoining the original sample container, indicating that they are in relation to a reference point Bequaert used (see section 3.2.). These two fragments were also selected for radiocarbon dating (Table 1). Finally, to further test the representativeness of charcoal radiocarbon dates for dating the age of pottery, we also directly radiocarbon dated a pottery fragment from *MUK1952* by scraping off flakes of soot from the outside of a sherd. As such, we selected a total of 16 samples for radiocarbon dating (13 from *MUK2018* and 3 from *MUK1952*) (Table 1). Radiocarbon dating was performed at the Royal Institute for Cultural Heritage radiocarbon dating laboratory (IRPA/KIK) using accelerator mass spectrometry (AMS) in a mini carbon dating system (MICADAS). For each radiocarbon date, the posterior probabilities for all calendar years were then calculated with the calibrate function in the rcarbon package in R (Bevan and Crema, 2022), using the SHcal20 calibration curve (Hogg et al., 2020).

### 3.5. Lithic refitting

Lithic refitting is to conjoin artefacts that are part of the same debitage (reduction by knapping) process and are, therefore, contemporaneous (Cahen, 1976; Cahen and Keeley, 1980; Romagnoli and Vaquero, 2019). There are, depending on various factors, different types of refits. Direct breaks of one flake into multiple segments (*Aneinanderpassungen*; Cziesla, 1990) are most common and can be caused by force emitted during knapping or post-depositional influences. The excavation method has to be considered for specific breakage types. In a direct flake break, a flake's proximal and distal parts can usually be joined again. The broken line is relatively straight; one might see where excavation tools applied force. Direct refits with a more uneven break-line, showing lips and other signs of kinetic force, hint at an occurrence during debitage (Hahn, 1989; Floss, 2012). Sequential refits (rejoining artefacts ventral to dorsal, thus reconstructing their reduction sequence) are most reliable for determining contemporaneity (*Aufeinanderpassungen;* Cziesla, 1990). They represent the reduction sequence of the nodule and temporal proximity during debitage. If sequential refits are found in long horizontal distances, surface movement can be considered. If sequential refits occur vertically over great length, it can hint at post-depositional vertical disturbances of the stratigraphy due to geomorphological or bioturbation events. Refitting creates spatial connections between the artefacts of the same refit set. Visualised as refit lines, these spatial connections allow to evaluate the impact of taphonomic processes on the spatial preservation of the site (Cziesla, 1990; Morrow, 1996; Villa, 1982). Refit analysis was performed for the vertical columns of *MUK2018* square 1 and *MUK1952* square *M* (Fig. 1). The macroscopically distinguishable raw material types (Fig. S7) were well-suited for a lithic refitting study. Refits were performed for pieces 2 cm and larger, as refit success rates in relation to time investment drop significantly for pieces smaller than 2 cm (Laughlin and Kelly, 2010).

**Table 1**
Calibration of AMS Radiocarbon dates from Mukila (calibrated using SHCal 20 curve cf. Hogg et al., 2020).

| LABNR | C14AGE | C14STD | D13C | SHCal20 | EXCAVATION | SQUARE | DEPTH | MATERIAL |
|---|---|---|---|---|---|---|---|---|
| RICH-26655 | 587 | 22 | −26.98 | 1325-1344 CE (10.3%)<br>1391-1434 CE (85.1%) | MUK2018 | 3c | 40–60 | *Elaeis guineensis endocarp* |
| RICH-26658 | 367 | 22 | −25.48 | 1484-1635 CE (95.4%) | MUK2018 | 2c | 40–60 | *Elaeis guineensis endocarp* |
| RICH-33107 | 413 | 24 | −25.5 | 1452-1512 CE (59.8%)<br>1548-1563 CE (3.2%)<br>1574-1624 CE (32.4%) | MUK1952 | J | ~66 | Soot |
| RICH-26656 | 1992 | 23 | −29.46 | 45-11 BCE (16.2%)<br>17-118 CE (79.3%) | MUK2018 | 2a | 60–80 | *Elaeis guineensis* |
| RICH-27381 | 3430 | 26 | −22.91 | 1868–1850 BCE (2.5%)<br>1771-1614 BCE (91.4%)<br>1560-1548 BCE (1.6%) | MUK2018 | 2b | 60–80 | Charcoal |
| RICH-27380 | 2176 | 25 | −23.83 | 350-312 BCE (14.8%)<br>195-90 BCE (76.4%)<br>83-65 BCE (4.2%) | MUK2018 | 1b | 80–100 | Charcoal |
| RICH-27410 | 3311 | 26 | −23.01 | 1621-1558 BCE (33.7%)<br>1550-1492 BCE (52.6%)<br>1483-1450 BCE (9.1%) | MUK2018 | 1c | 100–120 | Charcoal |
| RICH-30594 | 4581 | 34 | −21.3 | 3483-3475 BCE (0.9%)<br>3372-3098 BCE (94.6%) | MUK1952 | F-J | ~144 | Charcoal |
| RICH-26654 | 3347 | 25 | −28.14 | 1681-1657 BCE (2.1%)<br>1642-1502 BCE (93.3%) | MUK2018 | 1b | 140–160 | Charcoal |
| RICH-26657 | 4501 | 26 | −26.69 | 3342-3018 BCE (95.4%) | MUK2018 | 1c | 160–180 | Charcoal |
| RICH-30596 | 10103 | 59 | | 9890-9355 BCE (95.4%) | MUK2018 | 1a | 220–240 | Charcoal |
| RICH-27374 | 10098 | 33 | −26.77 | 9815-9657 BCE (43.6%)<br>9643-9551 BCE (21.3%)<br>9542-9373 BCE (30.6%) | MUK2018 | 1d | 280–300 | Charcoal |
| RICH-26653 | 12329 | 41 | −27.4 | 12.856–12.761 BCE (11.1%)<br>12.506–12.125 BCE (84.3%) | MUK2018 | 1a | 300–320 | Charcoal |
| RICH-27379 | 12268 | 37 | −24.95 | 12.368–12.097 BCE (94.5%) | MUK2018 | 1b | 340–360 | Charcoal |
| RICH-30595 | 32724 | 339 | −24.8 | 36.443–34.315 BCE (95.4%) | MUK1952 | M | ~445 | Charcoal |
| RICH-33715 | 37203 | 653 | −26.4 | 40.528–39.101 BCE (95.4%) | MUK2018 | 1b | 640–660 | Charcoal |

### 3.6. *Pottery analysis*

The ceramics found in *MUK2018* were systematically refitted to obtain vessel units, the basis for subsequent inventory study. Due to heavy fragmentation and low direct sherd joining rates (Fig. 5C), reasonable vessel units were thus defined based on the macroscopic fabric, shape and decoration of the sherds (Jesse, 2003: 81).

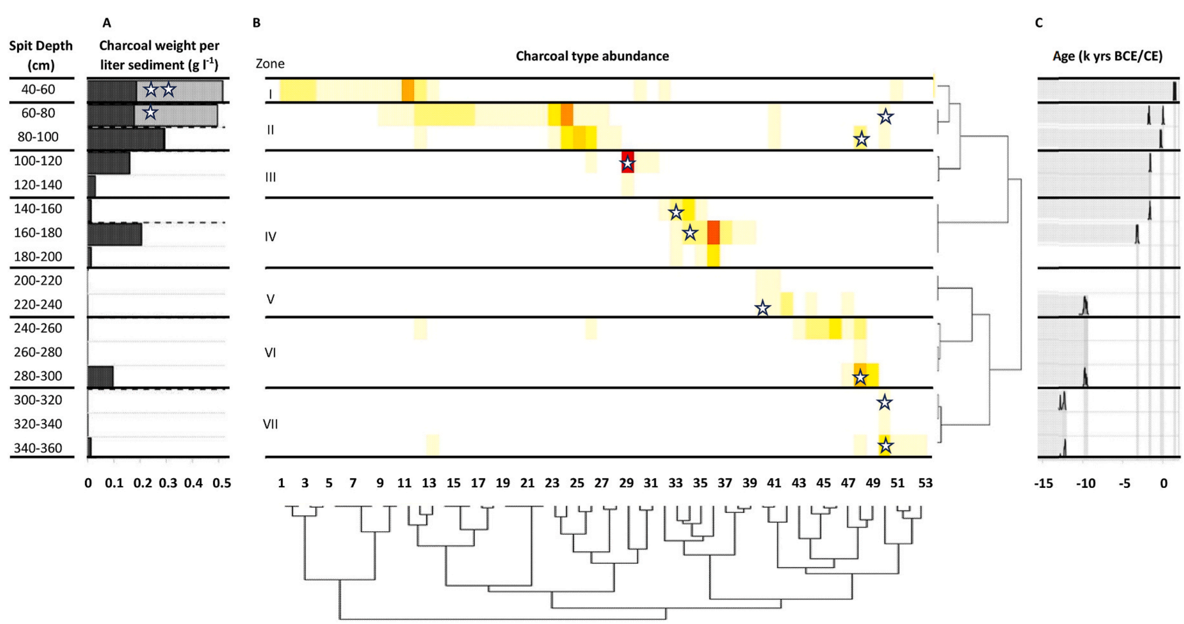


**Fig. 2.** Charcoal analysis of *MUK2018*. (**A**) Abundance of total charcoal mass per spit is expressed as charcoal weight per litre sediment (mg $l^{-1}$). Dark grey parts of the histogram represent wood-derived charcoal, and light-grey bars represent charcoal from oil palm endocarp. (**B**) Abundance of charcoal types per spit. The heat map represents charcoal abundance, with the darkest red representing the maximum number of charcoal fragments per type and spit and the lightest yellow representing the minimum number of charcoal fragments. The dendrograms result from constrained hierarchical clustering of spits (vertical dendrogram) and charcoal types (horizontal dendrogram). Based on the Mantel statistic, we found seven different depth zones, coded with Latin numbers I-VII and visualised throughout the graph with solid black horizontal lines. Charcoal types are indicated by their number between the heat map and the horizontal dendrogram (only odd numbers are displayed). (**C**) Age probability distribution of radiocarbon dates (in kyr BCE/CE). Radiocarbon-dated charcoal types are indicated with a star in panels A and B.

### 3.7. Grain size analysis

The grain size distribution was determined for 11 samples (Fig. 6B), each representing a 20 cm interval, collected every 60 cm between depths of 40–660 cm. Grain size analysis consisted of wet sieving at 63 µm, followed by dry sieving of the >63 µm fraction and applying the pipette method for the <63 µm fraction (van Reeuwijk, 2002).

## 4. Results

### 4.1. Charcoal analysis and radiocarbon dating

Clustering of charcoal types from *MUK2018* revealed a sequence of seven discrete zones (Fig. 2), five of which are characterised by an enunciated peak in charcoal mass. Distinctly different radiocarbon dates confirm the stratigraphy in charcoal mass and composition. Each of the five most abundant charcoal types identified down to genus level (Fig. S6; Tab. S1; Tab. S2) is dominant in one zone.

Zone I (40–60 cm) is characterised by a diverse composition of 15 charcoal types, with the dominating one being type 11 (22 fragments). Relatively abundant are types 1, 2 and 12 (each six fragments). This zone is also characterised by numerous charred endocarps, exclusively from oil palm (*Elaeis guineensis*). Two radiocarbon dates on palm endocarps place this zone within the 13th to early 16th century CE (RICH-26655, RICH-26658) (Fig. 2C). A date on soot from the outside of a sherd found in *MUK1952* dates to the mid-15th to early 17th century CE (RICH-33107). This date is directly connected to the pottery and its use. Type 11 was identified as cfr. *Vitex* spp. (Verbenaceae family). We refer to Table S1 for a complete anatomical description and Fig. S6 for Scanning Electron Micrographs (SEM). A diagnostic feature in this type is the semi-ring-porous vessel pattern (Fig. S6).

Zone II (60–100 cm) is characterised by an even more diverse composition of 19 charcoal types. Dominant charcoal taxa are type 24 (36 fragments), type 25 (19 fragments) and type 23 (13 fragments). The upper part of the zone especially carries an exceptional abundance of oil palm endocarps. Two radiocarbon dates place the zone in the 4th century BCE to 2nd century CE (RICH-26656 and RICH-27380) (Fig. 2C). Another radiocarbon date (RICH-27381) is much older, falling within the age range of Zone III. This mismatch might be due to post-depositional redistribution of some fragments, but this is the sole occurrence in a total of 16 radiocarbon dates. Type 24 is identified as cfr. *Julbernardia* spp. (Fabaceae family) (Fig. S6; Tab. S1).

Zone III (100–140 cm) is almost entirely dominated by a single charcoal type (type 29; 43 fragments) and contains no more oil palm endocarps. Radiocarbon dating indicates that the entire zone dates to the 17th to 15th century BCE (RICH-26654, RICH-27410) (Fig. 2C). Type 29 is identified as cfr. *Copaifera* spp. (Fabaceae family) (Fig. S6; Tab. S1).

Zone IV (140–200 cm) is primarily dominated by type 36 (42 samples), with type 34 (16 fragments), type 35 (5 fragments) and type 37 (5 fragments) also being abundant. This zone is characterised by a very distinct peak in charcoal abundance (160–180 cm, Fig. 2A) and dates to the 34th to 31st century BCE (RICH-26657) (Fig. 2C). Type 36 is identified as cfr. *Guibourtia* spp. (Fabaceae family) (Fig. S12; Tab. S1). A diagnostic feature of this type is the prominent presence of tangential lines of intercellular canals of traumatic origin (Fig. S6).

Zone V (200–240 cm) contains very few charcoal fragments, belonging to only three charcoal types. It dates to the second half of the 9th millennium BCE (RICH-30596) (Fig. 2C).

Zone VI (240–300 cm) is again characterised by a substantial number of charcoal types (9), dominated by type 48 (22 fragments) and type 49 (9 fragments). A discrete charcoal peak was uncovered in the lower part of the zone (280–300 cm). Like Zone V, this zone also dates to the 9th millennium BCE (RICH-27374) (Fig. 2C). Zones V and VI probably belong to the same period. Type 48 is identified as cfr. *Gilbertiodendron* spp. (Fabaceae family) (Fig. S6; Tab. S1).

Zone VII (300–360 cm) contains seven charcoal types and is dominated by type 50 (10 fragments). Interestingly, this zone also includes two endocarp fragments of *Canarium schweinfurthii*. Two concurrent radiocarbon dates, one from the upper part of the zone (RICH-26653) and one from the lower part (RICH-27379), date to the first half of the 13th millennium BCE (Fig. 2C).

The overall sequence of radiocarbon dates is based on 13 dates derived from our new excavation in 2018 and amended by three equally novel AMS dates that were done on legacy material from the 1952 excavation, showing an excellent stratigraphic order. Noteworthy is that two of the three dates on legacy material, one on legacy charcoals (RICH-30594) and one on soot from the exterior surface of a potsherd (RICH-33107), correspond to the 2018 dates from a similar depth. The date around the 37th to 35th millennium BCE (RICH-30595) on charcoal from the 1952 collection material has no equivalent among the 2018 charcoal samples, yet it is equally in good stratigraphic order (Fig. 2). Dates from the spits above are considerably younger (RICH-27379), and the date from the lowest level (RICH-37203) is significantly older. These novel radiocarbon dates from Mukila (Table 1) tentatively reconfirm a chronological gap during the late Pleistocene that has been previously identified and discussed (Cahen et al., 1983; Cornelissen, 2002, 2023). While there is still potential in bridging the chronological gap with organic material retrieved from the coring between 360 and 660 cm in 2018, we do not estimate the wider picture to change, as just 80 cm of sediment between 360 cm (RICH-27379) and 440 cm (RICH-30595) span more than 20.000 years (Fig. 3A). The potential of the site was tested up to 660 cm (RICH-33715) by including dates on material from the coring in 2018 and another from the excavation in 1952. So far, all currently available dates reconfirm the widely observed late Pleistocene gap event.

### 4.2. Lithic inventory from 2018 excavation

The excavation at Mukila École (*MUK2018*) revealed no clearly distinguishable archaeological horizons. The sediment comprises minimally varying colours of yellow-brown, slightly loamy sand (Fig. 6; S1). Without clearly separated visible sediment layers, analyses are based on the number of finds within the quadrant and artificial spits (Discamps et al., 2023). Extensive typo-technological analysis will be published elsewhere; the lithic industry is here strictly considered for its potential to assess site integrity by looking at find density (Table 2), size distributions (Fig. 3), raw material characteristics (Fig. S7) and refits (Fig. 4; S8). The excavation brought forth 7120 lithic artefacts. The number of artefacts decreases horizontally from square 1 to 3 and vertically down to roughly 300 cm below the surface, where it increases again in square 1 (Fig. 3C). While the upper 40 cm show numbers as high as 1500 pieces per quadrant (Table 2), they hold high percentages of debris not attributed to controlled, systematic tool-knapping (Whittaker, 1994) and, thus, are likely the result of the lithic sources being used in the construction of the church and the adjacent school buildings during the early 20th century. Furthermore, the upper 40 cm were mixed with modern materials such as plastic objects and glass fragments, therefore viewed as disturbed.

The total lithics in square 1 (a-d) count 4793, and the spits below 60 cm show no apparent signs of disturbance, such as bioturbation or pits (Fig. S1). The lithics from <60 to 660 cm amount to 381 objects, and 90% are smaller than 2 cm (Fig. 3C). Larger diagnostic pieces include flakes, retouched pieces, hammerstones, blanks and angular debris. The tools include scrapers, a point, a biface, blades and borers (Fig. S9). Flakes larger than 2 cm consist of an even mixture of end-struck and side-struck. A finely retouched bifacial point was found at 360 cm (Fig. S9:15). However, the low number of larger flakes and absence of cores in square 1 do not permit analysis of the temporal evolution of technological features.

A maximum of eight zones are visible within the lithic distribution in square 1 (Table 2).

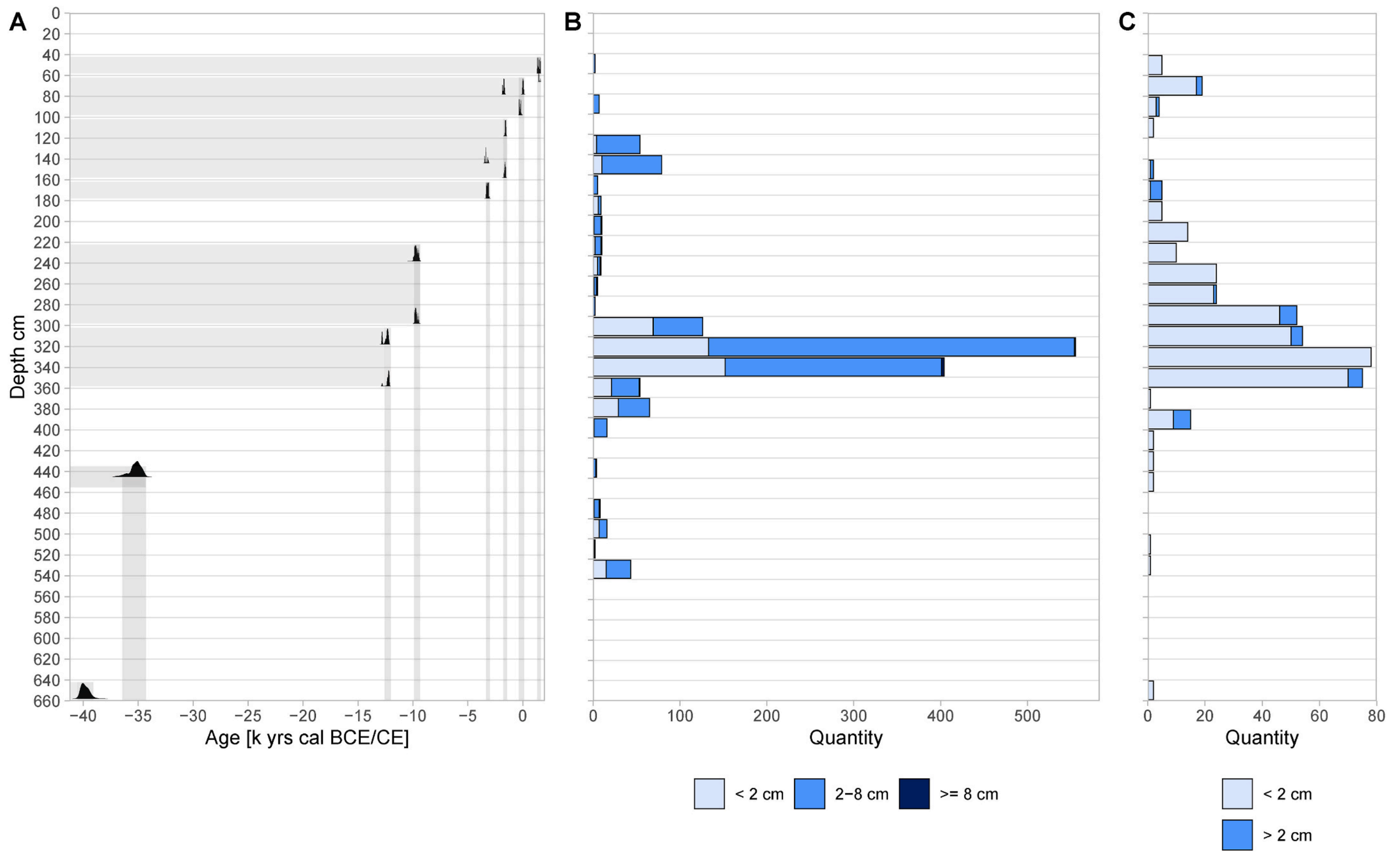


**Fig. 3.** Radiocarbon chronology (**A**) and distribution of lithics (total amount per spit) from *MUK1952*, square M (**B**) and *MUK2018*, square 1 (**C**). Shades of blue represent lithic artefact size distribution.

**0–60 cm**: The upper 40 cm are disturbed throughout the squares and quadrants. The recovered stones are of local material; however, few display traces of debitage. Although a small number of flakes, flake fragments, bladelets and angular debris exist, especially at 40 cm, the first two spits are also admixed with modern materials like glass and plastic fragments, as well as mortar equivalent to the one in the buildings. Additionally, rounded pieces occur consistently throughout the quadrants, making post-depositional movement in these two spits very likely. Interviews with the local community revealed that the church and school buildings (Fig. 1C) were constructed in the 1930s. The quadrants 1*a* and 1*b* are disturbed by a 2016 water pipe dugout (Table 2; Fig. S1), whereas 1*c* and 1*d* at 60 cm are undisturbed but only count five lithics (angular debris < 2 cm). A coin from 1947 was found at 20 cm, and the 60 cm spit is radiocarbon-dated to the 16th century CE (Table 1).

≥**60–100 cm**: The spit at 60–80 cm below the surface falls to the first century CE, constituting a chronological gap of 1500 years from the above spit (Fig. 3; Table 1). Mostly chips and few flakes occur between 60 and 100 cm (1b/100 cortical quartz flake, Fig. S9:10; 1d/100 side-struck silcrete flake). Below 80 cm, the artefact count drops drastically (Table 2). The spits date from the mid-first century CE (RICH-26656) to the fourth century BCE (RICH-27380).

≥**100–160 cm**: There is a complete lack of stone implements at 140 cm in all quadrants (Table 2). Quadrant *a* is empty from 100 to 160 cm, while *b* holds one artefact at 160 cm (hammerstone, Fig. S9:17). Quadrants *c* is equally empty, while *d* only provides three objects smaller than 2 cm (2 chips <1 cm, angular debris <2 cm). The spits at 120 and 160 cm date to the mid-2nd millennium BCE (RICH-26654, RICH-27410).

≥**160–300 cm**: Below 160 cm, artefact counts increase in all quadrants. This part can be subdivided into three subsections (>160–200, >200–240, >240–300 cm) with slowly rising artefact abundance. Findnumbers remain below ten individual pieces per quadrant until 240 cm (Table 2). Except for some implements (1a/180 blade, Fig. S9:2; 1b/180 borer, Fig. S9:13; 1c/180 blade and hammerstone, Fig. S9:4,18; 1a/200 angular debris; 1c/260 angular debris; 1d/260 flake; 1b/280 blade, Fig. S9:1; 1d/300 flake; 1b/300 siret break, Fig. S9:7; 1c/300 proximal flake fragment and cortical flake, Fig. S9:9), all are chips and cortex smaller than 2 cm. The 220 and 240 cm spits exclusively hold chips, mostly below 1 cm in size. Quadrant 1*d* at 300 cm already introduces the stark rise in artefact abundance seen below 300 cm. The spit at 180 cm dates to the late 4th millennium BCE, while the spits >220–300 cm date to the 10th millennium BCE (Table 1).

≥**300–360 cm**: The picture drastically shifts below 300 cm, where numbers per quadrant rise to more than sixty pieces, though still constituted by a majority of chips (95% < 2 cm). There is a stark increase of lithic abundance between 320 and 360 cm (Table 2), even though only quadrants *a* and *b* were excavated. The pieces larger than 2 cm comprise three flakes (Fig. S9:3,8), three angular debris, a borer (Fig. S9:12), a scraper (Fig. S9:19), a Stage 2 biface (Fig. S9:14) and a finely retouched (Stage 4) bifacial point (Fig. S9:15). The spits from <300 to 360 cm are dated to the 13th millennium BCE (RICH-26653, RICH-27379).

≥**360–660 cm**: Below 360 cm, the sample size drops significantly due to excavation strategies of coring in alternate quadrants. Nonetheless, at 400 cm, six larger pieces were retrieved (1b/400 four flakes, Fig. S9:5,11; two angular debris); the rest of the finds are chips, angular debris and cortex fragments smaller than 2 cm. Until 660 cm, numbers do not exceed nine pieces per unit. A charcoal sample from 660 cm dates to the mid-41st to 40th millennium BCE (RICH-33715).

Almost all lithics are made of silcrete sandstone. There are only two small (<2 cm) quartz fragments (at 220 and 300 cm) and a quartz cortical flake (160 cm, Fig. S9:10).

**Table 2**
Number of lithic artefacts found within each quadrant of *MUK2018* square 1 attributed to the depth below the surface and correlated to AMS dates. Yellow-to-red shading represents an increase in artefact abundance, while grey shading represents modern disturbances.

| Age | Depth | 1a | 1b | 1c | 1d |
|---|---|---|---|---|---|
| c.1947 CE | 20 | 1032 | 533 | 1489 | 521 |
| c.1930 CE | 40 | 232 | 128 | 222 | 141 |
| 1325 - 1635 CE | 60 | 65 | 44 | | 5 |
| 45 BCE - 118 CE | 80 | 9 | 2 | 1 | |
| 350 - 65 BCE | 100 | | 1 | 2 | 1 |
| 1621 - 1450 BCE | 120 | | | | 2 |
| | 140 | | | | |
| 1681 - 1502 BCE | 160 | | 1 | | 1 |
| 3342 - 3018 BCE | 180 | 1 | 1 | 2 | 1 |
| | 200 | 2 | 1 | 2 | |
| | 220 | 3 | 7 | 2 | 2 |
| 9890 - 9355 BCE | 240 | 4 | 1 | 1 | 4 |
| | 260 | 5 | 4 | 10 | 5 |
| | 280 | 2 | 6 | 8 | 8 |
| 9815 - 9373 BCE | 300 | 10 | 7 | 11 | 23 |
| 12.856 - 12.125 BCE | 320 | 24 | 25 | | |
| | 340 | 61 | 14 | | |
| 12.368 - 12.097 BCE | 360 | 50 | 28 | | |
| | 380 | | 1 | | |
| | 400 | 9 | 6 | | |
| | 420 | | 2 | | |
| | 440 | 2 | | | |
| | 460 | | 2 | | |
| | 480 | | | | |
| | 500 | | | | |
| | 520 | 1 | | | |
| | 540 | | 1 | | |
| | 560 | | | | |
| | 580 | | | | |
| | 600 | | | | |
| | 620 | | | | |
| | 640 | | | | |
| 40.528 - 39.101 BCE | 660 | | 2 | | |

One sequential and one direct refit were possible within square 1 (Fig. 4B). Many chips (<2 cm) resemble bigger artefacts in raw material without direct refits. At 360 cm, a piece of angular debris of the same raw material joins ventral to dorsal onto the Stage 2 biface (Fig. S9:15). At 300 cm, two parts of a flake join (Fig. S9:6). All refit lines occur within the same 20 cm spit (Fig. 4B; S8C).

### 4.3. Lithic refitting in 1952 inventory

Near Mukila's school ('Mukila École'), Bequaert excavated an eleven-by-thirteen-metre large trench (*Gite II B*), subdivided into multiple squares (Fig. 1C, Fig. S2). His publications refer to the individual squares (Bequaert, 1956b: 35–37), but the spatial organisation of the units was never published. Bequaert's handwritten notes and photos of the situation are archived at the RMCA and help to contextualise his finds from Mukila (Fig. S3, S5). In 1952, his excavation of *Gite II B* (*MUK1952*) uncovered ceramic finds to 50 cm below the surface and lithic artefacts in distinct concentrations, starting at about 80 cm below the surface. The deepest point was reached in square "*M*", excavated to 680 cm below the surface. Bequaert noticed a considerable accumulation of lithics in the northern units at 80–120 cm below the surface. At 125–150 cm beneath the surface, a second concentration appeared in the northeastern units of the trench. Further down (190–210 cm), lithics were encountered on the northwestern and eastern edges of the trench. A fourth concentration was encountered between 300 and 380 cm below the surface in the south-easternmost units. The fifth was found in the central unit (*M*) between 450 and 540 cm below the surface (Fig. S10) (Bequaert, 1956c). The central square *M* constituted a roughly upside-down pyramid shape with a four-on-three metre base and irregular steppings (Fig. S2; S3; S10) to approximately 7 m. It is visible in the photographs and Bequaert's sketches that steps were made irregularly and with differing heights. Some steppings may have even been made after areas were already excavated deeper. The excavator attributed most of the 2495 lithics with a depth value below the surface. The documentation is rough but traceable; depth was mostly recorded, but spit sizes and the exact size of each stepping are challenging to discern.

Though Bequaert did not record sieving activities, he still collected a representative number of lithics of smaller dimensions, indicating that no sub-sampling was conducted on-site. Of the 1513 artefacts within the central column *M,* size distribution shows that 31% of objects are smaller than 2 cm, the majority (68%) are between 2 and 8 cm, and less than 1% are larger than 8 cm (Fig. 3). Of eleven artefacts larger than 8 cm, most could be considered hammer or grinding stones, and very few are bigger flakes, blades, and points, angular debris or cores (Fig. S11). Several raw material variations could be distinguished, though all *MUK1952* lithics are still made from locally occurring '*grès polymorph*', a silcrete sandstone formed by groundwater and mineralisation in sandy strata (Thiry and Milnes, 2017). The formation process is similar in all silcretes, and the local mineral composition leaves recognisable traces in colour and granulation during formation. Most variations have notable similarities, but minor differences can set them apart when closely examined and compared with their depositional depth (Fig. S7).

The lithics of both excavations correspond exceptionally well to the local polymorphic silcretes, also used in colonial buildings. A 2018 survey confirmed that the raw material used in ancient tools and modern buildings occurs locally (Seidensticker et al., 2018: 27 Fig. 5). These comparisons remain macroscopical (Tafelmaier et al., 2022) and have not yet been chemically verified. As silcrete sandstone is widely distributed in Central and Southern Africa, a more detailed differentiation at the typological and geochemical levels is necessary to better understand raw material procurement and selection. For decades, much of the Central African raw material (*grès polymorph*) was deemed too tricky to differentiate (Cornelissen, 2003). As examples from Southern Africa show, contrary to common belief in Central African archaeology, even silcrete polymorphic raw materials can be chemically distinguished. Sources of tools were individually identifiable by allowing the distinguishing of specific silcrete outcrops and indicating long-distance transport (Nash et al., 2013; Schmidt et al., 2021).

The central and deepest square *M* from *MUK1952* was chosen for the refit analysis, emitting lithics <2 cm (Laughlin and Kelly, 2010). A total of 62 lithics from *M* could be refitted, corresponding to 4.2% of its artefacts. No complete reduction sequence could be determined by refitting column *M*. No refits occurred between different silcrete variations. Some refits could be identified as modern breaks, as they occurred after labelling or inventory numbers were applied to the pieces. Some breaks happened post-excavation but before inventory numbers were applied. Thus, it was not broken pre-depositionally or in situ. Several direct refits of proximal and distal flake ends show medial pressure application visible in breaks caused by modern excavation tools (Fig. S12:2–4). This modern break represents recording errors common for excavations before the 1970s/80s. This amounts to a total number of 22 artefacts that were excluded from further study due to their modern breaks.

Direct refits (48%) and sequential refits (52%) occur in relatively equal numbers among the remaining artefacts. The refit lines are largely short-distance, with 82% occurring within a vertical span of fewer than 20 cm, often at the exact same depth. Three sequential refits between 180 and 260 cm (Fig. 4A) are from the same hypothetical nodule, showing the same raw material and a distinct patina (Fig. S12:9,12).

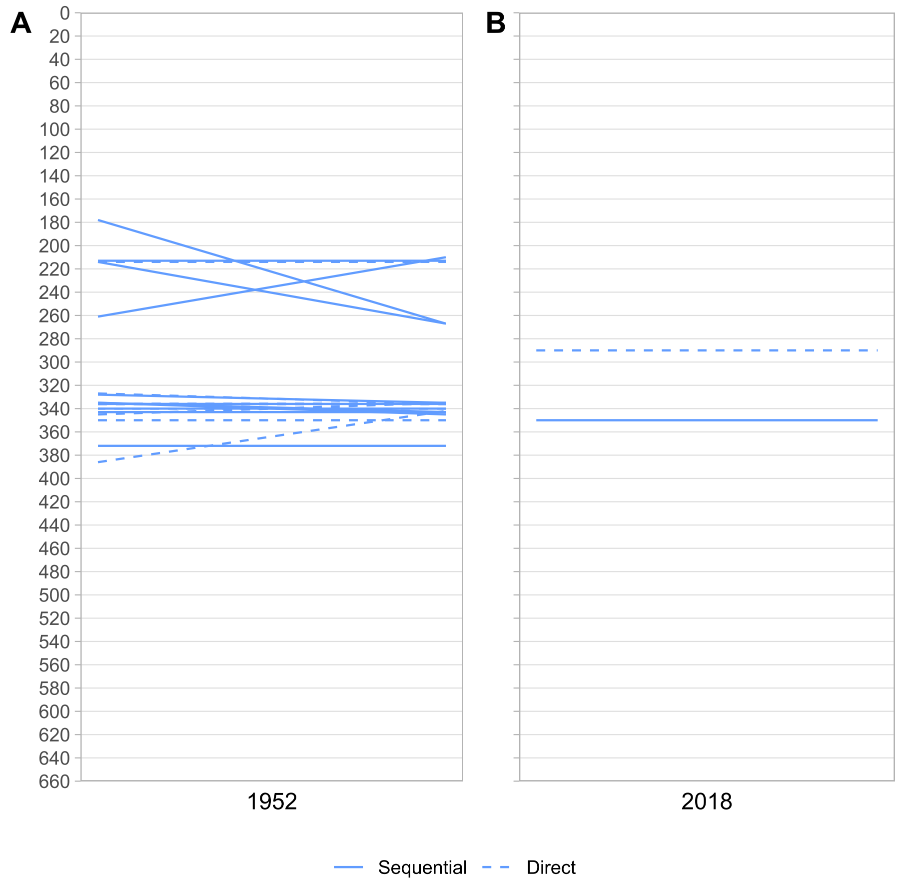


**Fig. 4.** Refits found among *MUK1952* (**A**) and *MUK2018* (**B**) lithics. For square *M* (*MUK1952*), 64 artefacts (4.2%) were refitted, and four artefacts (1%) could be refitted in square 1 (MUK 2018). Each line represents refits of at least two pieces. These are subdivided into modern breaks (clearly in-/post-excavation), direct refits (joining of proximal and distal ends of one artefact) and sequential refits (joining minimum of two artefacts ventral to dorsal). Refer to Fig. S8 for a comparison with radiocarbon dates, botanical zones and lithic abundance.

These three sequential refit lines transgress the boundaries of the botanical zoning (Fig. S8D). Two directly refitted artefacts from that same nodule were found at the same depth (Fig. 4A, direct refit), which equally applies to a sequential refit from another nodule (Fig. S8B). Thus, not all artefacts from 180 to 260 cm are equally disturbed. Of a total of 9 artefacts in that interval, 55% were disturbed. Of the two refitted sets with three artefacts (Fig. S8D), one (Fig. S12:12) does, and the other (Fig. S12:10) does not transgress zones. Generally, the majority (82%) of all refits do not transgress botanical zone boundaries. Additionally, we see no such disturbances between 320 and 380 cm (Fig. 4A; S8B), where the majority of refits and a large number of sequential refits (cf. Fig. S12:10 refit in Fig. 4A/S8 at 340 cm) occur.

There are no stratigraphic indicators as to why the refit length patterns vary substantially at 180–260 cm compared to 320–380 cm (Fig. 4, S8). The homogeneity of the sediment body (cf. Section 4.5) did not allow for the differentiation of in-field layers in 2018, and the documentation from 1952 is equally void of lithological indicators.

### *4.4. Pottery description and refitting*

The collection of ceramics from *MUK1952* comprises 484 sherds, while *MUK2018* yielded 611 sherds (Fig. 5). Systematic sieving resulted in 90 sherds per sqm in *MUK2018* (6.75 sqm), compared to three sherds per sqm in *MUK1952* (~150 sqm). Bequaert regularly encountered pottery to 80 cm below the surface (97 %, Fig. 5A). Six sherds (2 %) were found below that, and the depth of four sherds (1 %) could not be reconstructed. In *MUK2018*, most ceramics were found above 60 cm (96 %), and the spit from 40 to 60 cm held nearly half of all ceramics (46 %, Fig. 5B). This spit dates to the 13th to early 16th century CE (RICH-26655, RICH-26658). Refitting sherds to obtain vessel units showed considerable horizontal but minimal vertical admixture (Fig. 5C), corresponding to the observed disturbances in the upper 60 cm. Both inventories are highly fragmented, and undecorated wall fragments are most abundant (*MUK1952*: 82 %; *MUK2018*: 95 %).

The Mukila ceramics exhibit considerable heterogeneity in terms of macroscopic fabrics. Most sherds have either a light grey/beige or reddish surface colour, and macroscopically visible inclusions are often heterogeneous mixtures of quartz particles with few organic remains. Notably distinct fabrics contain slag (*MUK1952* & *MUK2018*: 11 %) or grog tempering (*MUK1952*: 5 %; *MUK2018*: 3 %). Fine ware with whitish surface colour and no macroscopically discernible non-plastic particles, similar to the pottery common to the Inner Congo Basin (Seidensticker, 2016, 2021), rarely occur (*MUK1952*: 0.4 %; *MUK2018*: 3 %). Most noteworthy is a small group of sherds (*MUK1952*: 3 %) that contain tiny silcrete chips, the raw material of the site's lithics (Fig. S7: C2, K, & N).

Only 10 % (*MUK2018*) to 15 % (*MUK1952*) of sherds show decoration. Simple grooves or comb impressions prevail, and patterns are horizontal or festoon-like. Decorations are solely placed below the rim or on the shoulder. An equal number of sherds show diagnostic vessel shapes (*MUK1952*: 13 %; *MUK2018*: 10 %). The most common types are globular pots with everted rims, straight lips and convex shoulder parts (Fig. S13; S14).

In summary, the ceramic inventory consists of undecorated or sparsely decorated vessels with convex bellies and everted rims, often lacking a distinct neck. The considerable lack of regional comparative

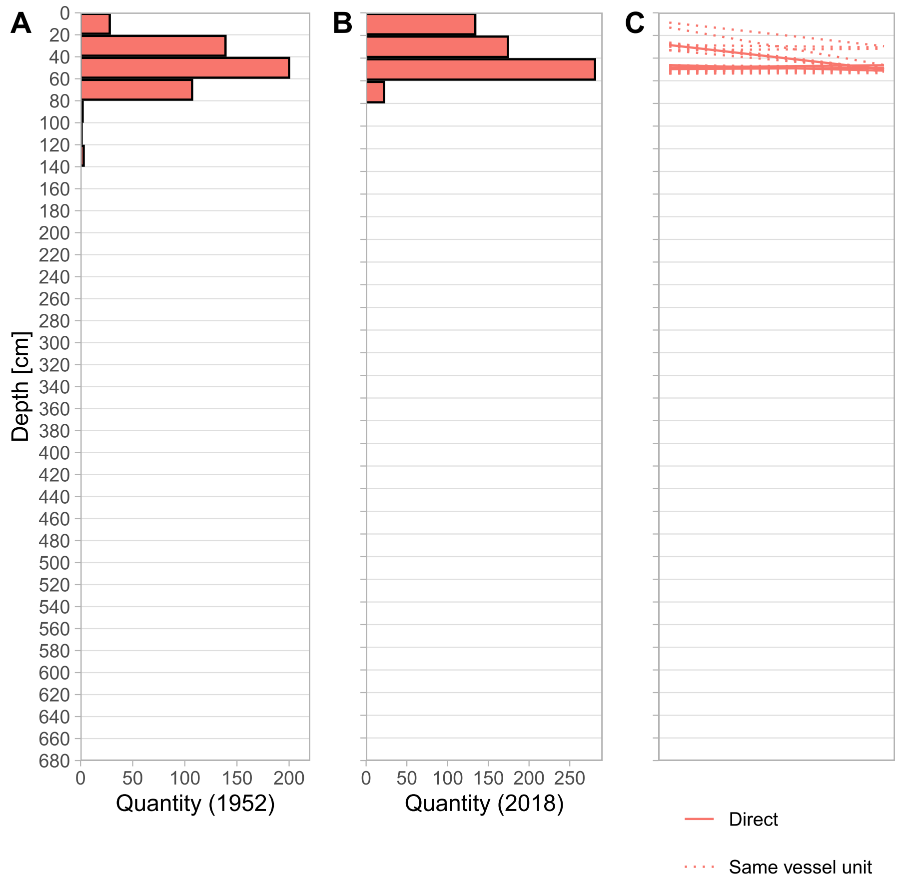


**Fig. 5.** Vertical distribution of pottery finds in *MUK1952* (**A**) and 2018 (**B**) as well as refits (**C**). A solid line marks two directly joined sherds, while a dotted line marks cumulated sherds to a vessel unit (based on the macroscopic fabric, shape, and decoration of the sherds).

material impairs the definition of any specific type. Only the inventories of other excavations conducted by Bequaert in 1952 in the vicinity of Mukila yielded similar pottery, all of which still need to be dated, such as Mukambo and Makongo, located south of Mukila. The inventories of all three sites show similar fabrics and are dominated by globular pots with short, everted rims (Fig. S14). Decorations consist of different versions of grooves in zigzag or wavy motives and diagonal comb impressions, surrounded by bands of horizontal grooves.

One of the novel radiocarbon dates from 60 cm below the surface at Mukila dates to the late 15th to early 17th century CE (RICH-26658), while the second date from that spit is slightly older (RICH-26655). A third date, obtained from soot sticking to the outside of a sherd from *MUK1952* (RICH-33107), dates between the other two. Thus, the ceramic inventory uncovered at *MUK1952* and *MUK2018* can be confidently dated from the 14th to early 17th century CE. The vessel shapes and decoration system observed at Mukila is reminiscent of the type B pottery of the Kongo Kingdom (Clist et al., 2018: 260–261 Fig. 19.17:8), formerly designated *Groupe V* by Mortelmans (1962a & b). Only the orientation of the rim is slightly different. While vessels of type B of the Kongo Kingdom pottery show horizontally flattened rims, all rims observed at Mukila are usually everted. One vessel from the hilltop of Mukambo showed the typically flattened rim of the type B pottery. The available radiocarbon dates for this ceramic type cover the late 16th to 18th century CE (Clist et al., 2018: 261).

Among the diagnostic pieces are bowls with plastic ledges on the broadest diameter (Fig. S10:20). This type also occurs at Makongo (Fig. S14:10–11). Another vessel unit with a pronounced carination (Fig. S13:18) resembles a sherd from the site of Dundo airfield, in north-eastern Angola (~500 km south-east of Mukila), dated to the end of the 7th to early 11th century CE (UCLA-716; Clark, 1968: 201 Pl. 2.2). The closest site towards the east is Mashita Mbanza (de Maret, 1982: 84), about 220 km eastwards of Mukila. It yielded only Later Iron Age pottery dating to the 16th to 20th century CE (Pierot, 1987), and its inventory consists of funnel beakers showing round bases, carinated walls and quite long, slightly everted rims decorated with horizontal and vertical parallel grooves or tracing (Cranshof et al., 2018: 194). None of the pottery from Mukila resembles this type. The described characteristics of the Mukila pottery are reminiscent of the Kongo Type B; the overall vessel shapes, techniques, and decoration motives match, and only the rims are shaped slightly differently.

### 4.5. Grain size distribution

Granulometric analysis revealed an extremely uniform grain size distribution throughout the profile despite marginal shifts in colouration (Fig. 6). The sediment has a loamy sand texture, with a very limited range of silt and clay contents (5–9% silt, 6–11% clay), which are only marginally higher in the lower half of the profile (Fig. 6B). In addition, the size distribution of the sand fraction is highly uniform. As calculated for the 20–63 to 355–500 μm fractions, the arithmetic mean varies narrowly between ca. 167 and 179 μm, with a ca. 173 μm average. This fine sand is consistently moderately sorted, with symmetrical distribution and mainly mesokurtic kurtosis. The granulometric characteristics are quite similar to those for the *Série des Sables Ocre* deposits that were analysed by De Ploey et al. (1968), except for an often much higher clay content (commonly >20%). As argued by those authors, the relatively poor degree of sorting is not clearly compatible with aeolian sedimentation. The highly uniform grain size distribution in the Mukila profile

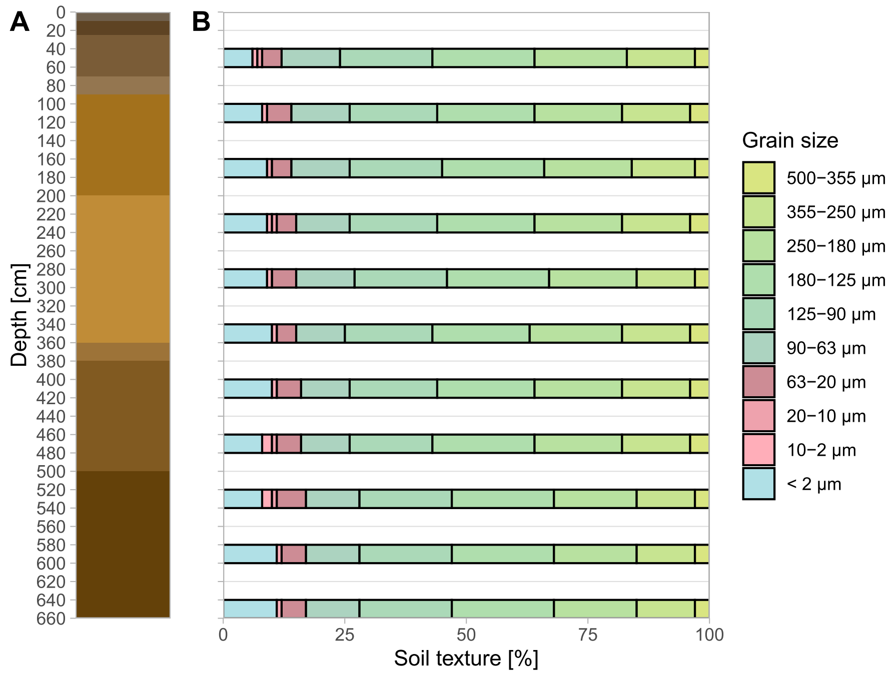


**Fig. 6.** Munsell soil colours (**A**) and grain size distribution (**B**) in *MUK2018*. Soil colours 0–360 cm were determined on the archaeological profile, while colours below were determined from soil samples collected during coring. While marginal colouration differences occur at various depths, it is important to stress that sediment composition does not significantly change over more than 6 m.

records either excellent stability of sediment accumulation conditions over the period recorded by the profile or must be attributed to post-depositional processes that resulted in complete uniformisation. The stability of the depositional environment is most compatible with a short period of sediment accumulation, but radiocarbon dating indicates that the deposits formed over 40000 years, with likely interruptions in sedimentation. Post-depositional uniformisation by soil fauna, slope processes, or human activity is incompatible with the seemingly unmodified vertical sequences recorded by charcoal fragments and lithic material unless the involved processes left relatively coarse-grained components unaffected.

## 5. Discussion

### 5.1. *Post-depositional disturbances in sites along the Kalahari Sand Belt*

One of the primary reference sequences for the Pleistocene and Holocene lithic industries in Central Africa has been the site of Gombe (Cahen, 1976; Cahen et al., 1983; de Maret and Stainier, 1999; Taylor, 2011, 2022). Discrepancies in the chronometric dates from the 1970s must be partially associated with a sampling method of ‘scattered’ and ‘concentrated’ charred remains (Cahen et al., 1983, p. 444 Table 1A). An extensive lithic refitting program aimed at reconstructing technological behaviour (Cahen, 1976, 1978), but found that artefacts crossed the established industries. The conclusions of massive vertical disturbances of archaeological materials had severe implications for interpreting the site’s integrity. It was concluded that no direct relationship was to be established between a radiocarbon date and artefacts at the same level.

Further examples of comparable stratigraphic contexts were observed in similar conditions from the North-East of Angola and the South-East in Katanga, including the Dinga Kiitu site (Bequaert, 1952, 1955, 1956a). Mixed and blurred stratigraphic contexts of the Late Pleistocene into the Holocene were assumed to be related to the same perturbation processes observed at Gombe. Thus, the standing conclusion was that “the redistribution [of archaeological material] has a general and systematic character in the entire area covered by Kalahari-type sands in Central Africa” (Cahen and Moeyersons, 1977, p. 814). It discouraged archaeological research covering the Pleistocene periods, particularly regarding the entire region’s Lupemban and Tshitolian, and all previously identified industries were grouped into the Post-Acheulean Complex (Cahen, 1978, pp. 21–22).

As a general hypothesis, it was assumed that objects were moving down within the unconsolidated sands of the Kalahari Belt, and, thus, concentrations of archaeological finds were disturbed through time. Experiments studying subsurface movements and dispersion of artefacts found that penetration can be driven by wetting-drying cycles due to slight compressions of sediment beneath objects (Cahen and Moeyersons, 1977; Moeyersons, 1978). This effect is dampened by increasing depth, and thus general consolidation, and becomes negligible after a certain depth. Potential differences in descending ‘velocities’ between stone artefacts compared to charcoal concentrations are unknown. The potential of anthracological charcoal analyses to provide stratigraphic and environmental units by displaying species variability was not explored during the Gombe reassessment in the 1970s.

### 5.2. *Stratigraphic integrity at Mukila*

Our integrated results (Fig. 7) underline that the sequence of archaeological finds at Mukila is mainly undisturbed. We approached our assessment of the site’s integrity based on multiple lines of reasoning.

The phases observed within the newly obtained AMS radiocarbon dates clearly show distinguishable groupings of dates falling into the same period (Table 1; Fig. 2C; 3A; 7A). Chronological phases are separated by 1500–2000 years on average, except for one larger recess within the sequence from the 4th to 9th millennium BCE (Table 1). Changes in the lithic artefact distribution largely correspond to shifts in radiocarbon dates (Table 2).

Furthermore, the anthracological analysis shows seven distinct zones with a different charcoal-type composition (Fig. 2B; 7B; Fig. S6). Dominant charcoal types occur only within their respective zone, corroborating the existence of discernible zones.

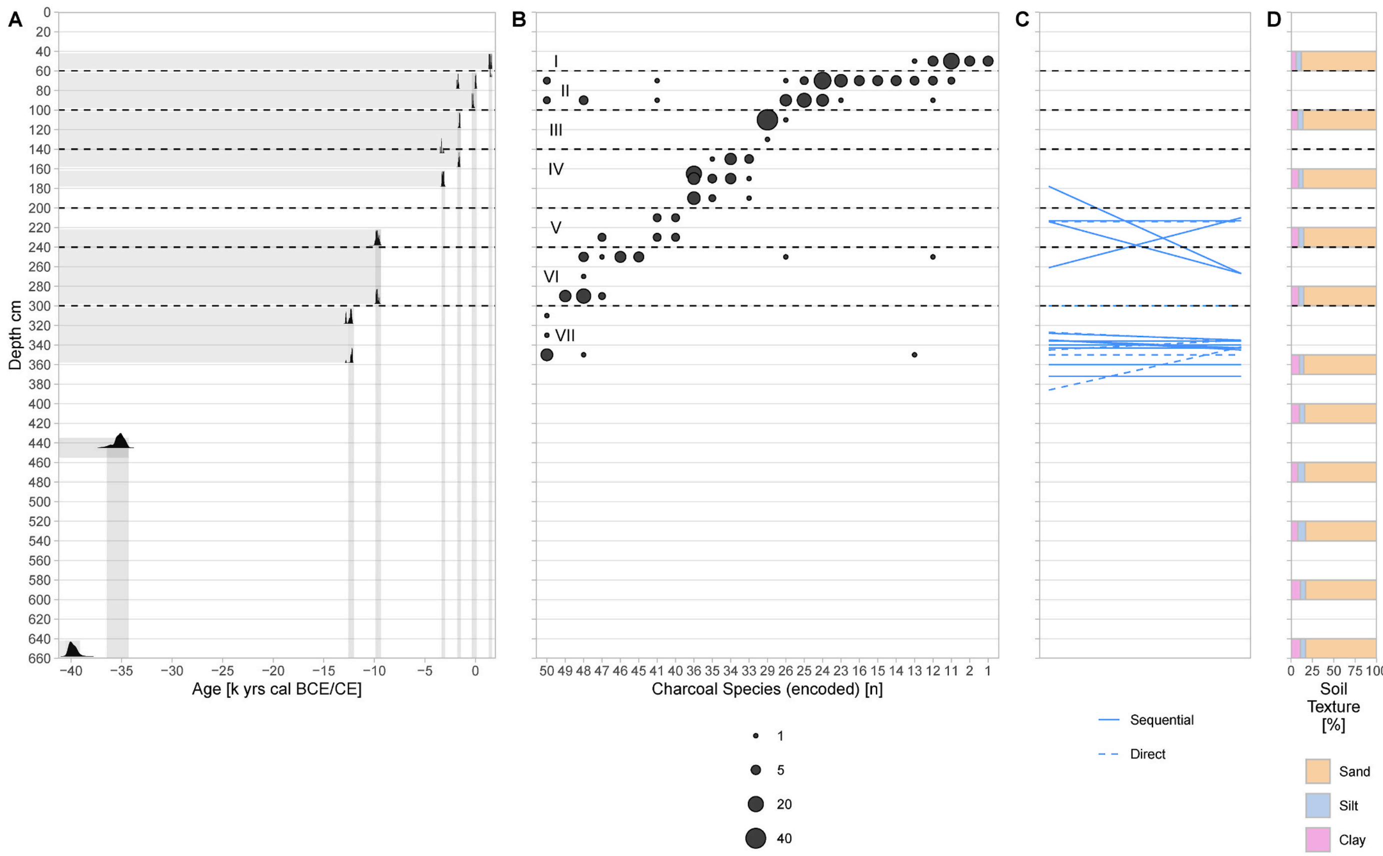


**Fig. 7.** Summary of results from the excavation *MUK2018* and the refitting of *MUK1952*: (**A**) Radiocarbon chronology. In light grey dates from *MUK1952*; (**B**) Distribution of (encoded) charcoal types. Only types found more than five times within the entire assemblage are plotted. The complete list can be found in Fig. 2. Dashed horizontal lines indicate significantly different depth zones found by constrained hierarchical clustering analysis on the charcoal type abundance data. They have been extended to the other panels as stratigraphic units; (**C**) Refits found among the lithics in *MUK1952* and *MUK2018*; (**D**) Granulometric analysis.

The vertical find distribution in *MUK1952* and *MUK2018* revealed multiple peaks in lithic abundance (Fig. 3), with a clear extreme in lithic abundance around 340–360 cm in both excavations. Artefact shatter (<0.5 cm) exists in all spits of *MUK2018*, and we did not encounter any correlation between the artefact size and its depth. One would imagine the size distribution to be more sorted by depth if the occurring pattern was solely the product of "sinking" artefacts in unconsolidated sand (Cahen and Moeyersons, 1977; Moeyersons, 1978).

The lithic refitting results (Fig. 4A; **7C**) show variations within the sequence, with isolated, long-distant refits only observed between 180 and 260 cm below the surface. These longer vertical refit lines occur among surprisingly few finds at this depth (Fig. 3B). In contrast, the 320–360 cm layers show considerably less vertical admixture amidst the main concentrations of lithics (Fig. 3B). The vertical extent of 82% of direct and sequential refit lines is below 20 cm on average and thus highly supports good stratigraphical integrity.

The pedogenetic processes leading to this stratigraphy are yet to be established. We do not consider erosion and subsequent colluvial deposition as the driver of the observed admixtures between 180 and 260 cm. A working hypothesis in which sediments and finds would have been collated by colluvial deposition from a higher part of the hill would have to entail a significant proportion of horizontal distribution coupled with a vertical component. Taking into account that the finds from square *M* of *MUK1952* originate from a unit of 12 sqm in size, the smaller number of artefacts, and the limited number of refits (n = 9) found between 180 and 260 cm, we conclude that the main driver of the observed displacement in that part of the sequence was a process working in the vertical axis exclusively. The experimental study dealing with vertical displacements at the site of Gombe by Cahen and Moeyersons (1977; Moeyersons, 1978) proposed vertical displacement due to wetting-drying cycles. We hypothesise that the intensity of wetting-drying cycles is coupled with the type of vegetation present at a site. Changes in the intensity of vertical displacement through time might, thus, reflect changes in vegetation cover and, subsequently, soil saturation by rainwater.

Concerning the site formation processes at Mukila, we can only offer hypotheses based on the available data. Especially challenging is the reconciliation of the sediment data, showing a striking uniformity in grain size (Fig. 7D), with all other data available from the site, which display distinct zonation (Figs. 2–3, 7A-C). The homogeneity in the granulometric data on its own would suggest that the sediments were deposited over a short period, which is contradicted by the radiocarbon-dating results (Table 1). A long period of sediment accumulation, of up to 40000 years would imply exceptional stability of sedimentation process and conditions. The disparity between sediment homogeneity and zonation of the coarser charcoal and artefact fractions indicates that these two components underwent different processes. A working hypothesis is that the sediment matrix was reworked after deposition, e.g. through bioturbation, while the same processes left all coarser components largely unaffected. However, based on the available field data, this hypothesis remains untested.

In summary, clear segments can be distinguished within the archaeological, radiocarbon dating and anthracological sequences at Mukila and show only confined vertical displacement of singular objects, while the majority of refits (82%) remain at the same depth. We interpret these chronological and spatial aggregations to represent multi-phased occupation sequences and subsequent soil consolidation at the site. The exact site formation process is uncertain as the astonishingly uniform distribution of grain sizes (Fig. 7D) challenges aeolian deposition.

The coherence in Mukila's stratigraphy has an essential impact on assessing the validity and representativeness of open-air sites. Moreover, it also illustrates the potential of palaeoecological research using charcoals as a stratigraphic proxy. While established palaeoecological proxies such as stratified marine, freshwater or peat deposits are rare in Central Africa (Nash et al., 2016; Hawthorne et al., 2023), charcoals are omnipresent (Hubau et al., 2015; Hart et al., 1996; Vleminckx et al., 2014; Hubau et al., 2015; Morin-Rivat et al., 2014) and easy to sample. Hubau et al. (2015) demonstrated that even locations with no archaeological artefacts revealed remarkable site integrity, expressed in distinct charcoal assemblages of separate types corroborated by radiocarbon dating. Even in sandy environments like Mukila, charcoal analysis is a promising tool to assess the integrity of sites void of visible lithological units and further unravel the Central African paleoenvironment and archaeological contexts. While stratified open-air sites are rare in Central Africa (Mercader and Martí, 2003; Peyrot et al., 2003; Oslisly et al., 2006; Mesfin et al., 2021), the examination of Mukila revealed that prior generalisations concerning vertical disturbances (Cahen and Moeyersons, 1977) might not apply to all sites and could be refuted by careful examination of post-excavation stratigraphies. While critical evaluation of field layers is more commonly performed for cave sites (Staurset and Coulson, 2014; Clarkson et al., 2017), our research shows the equal importance of these analyses for open-air sites.

While research on open-air sites in wider Africa often focuses on overall site-formation processes amidst clearly discernible sedimentary bodies (Kent and Scholtz, 2003; Wright et al., 2017; Phillips et al., 2023), few sites in Central Africa, contemporaneous to Mukila, regularly depict distinct lithological units (Mercader and Martí, 2003; Mesfin et al., 2021). The debate on post-excavation stratigraphies is new, though Discamps et al. (2023) point out that revising stratigraphies after excavation has been more common than acknowledged. Lithological observations in the field are often re-evaluated during subsequent analysis of artefacts, their distribution, typology, etc. In the case of Mukila, a very uniform and homogenous sediment body did not lead to apparent friction between artefact distribution and observable zoning. Thus, all implications towards a revision of an observed stratigraphy are absent. However, using charcoals and lithics, the identification of meaningful zones was possible. This differs from previously presented sites such as Gombe (Cahen, 1976; Cahen et al., 1983) in that Mukila needed a post-excavation stratigraphic framework to be interpretable. The implications of these results on the debate of post-excavation stratigraphy are, at best, that sedimentology may not be the most essential factor when reconstructing chronological phases at archaeological sites. However, more importantly, the implications for the research on open-air sites in Central Africa are much more severe in that this example produces an antithesis to the prevalent picture of the uninterpretable nature of sandy open-air palaeolithic sites.

### 5.3. Latest LSA and early Iron Age

The Late Stone Age (LSA) is primarily defined for Eastern and Southern Africa (Ambrose, 1998; Wadley, 1993). The South African terminology was adopted for LSA lithic industries in Central Africa, previously called Tshitolian (Lanfranchi, 1987; Miller, 2001). The Pleistocene part of the LSA in Central Africa is relatively well described at Shum Laka (Cornelissen, 1996, 2003; Lavachery, 1996, 1997, 2001). In contrast, the younger LSA industries are understudied or disregarded in favour of newly introduced ceramics and need to be studied better (Lavachery, 1990). For the younger industries of the Central African LSA, no general typological framework exists so far, and there is little comparable material. In South Africa, "a Wilton Industry date [s from the 6th to 4th millennium BCE] and a pre-ceramic post-classic Wilton date [s to the turn of times]" (Wadley, 2000:90), thus defining the latest LSA for Southern Africa.

For Central Africa, however, the general lack of sites makes "it [ …] problematic, if not impossible, to define a Late Stone Age in the Central African rainforest" (Eggert, 2019:75). Tshitolian sites in the Republic of the Congo and Gabon have been dated to the beginning of the Holocene (Lanfranchi and Schwartz, 1990). The Tshitolian sites of Cauma, Dinga Kiitu, Lobeja-Kabala, Mbalambala, Bena Tshitolo and Mukambo lie dispersed in an area that stretches over the DRC and Angola (Miller, 1988, 2001). Besides Gombe (Cahen, 1976; Cahen et al., 1983) and an undated site called 'Plateau the Batéké' east of Kinshasa (Cahen and Mortelmans, 1973), open-air sites with long sequences (covering the entire LSA) are very rare. Examples are Lopé 2 (Peyrot et al., 2003) and Maboué 5 in Gabon (Oslisly et al., 2006; Mesfin et al., 2021), and Njuinye in Equatorial Guinea (Mercader and Martí, 2003). Other lithic sites, such as Bandundu in the DRC (Seidensticker et al., 2018), lie roughly 200 km north of Mukila but are neither dated nor typologically described. Moreover, sites with both contemporaneous latest LSA lithics and Early Iron Age (EIA) pottery are even scarcer (Jungnickel, in prep.). The site of Bwambé in south-eastern Cameroon yielded mainly pottery dating into the 1st millennium BCE but also some lithics (Eggert et al., 2006), whose exact correlations still need to be established (Jungnickel, in prep.). The Tshitolian/LSA in Central Africa is considered to have ended around the turn of time with the introduction of Iron Age technology (Miller, 2001). In some parts, hunter-gatherers supposedly took refuge in more remote areas throughout a millennium (Miller, 1969). Additionally, due to the disturbances at Gombe, Stone Age cave sites were usually preferred for the study of temporal development (Emphoux, 1970; van Noten, 1977; de Bayle des Hermens and Lanfranchi, 1978; de Maret, 1986; Lavachery et al., 2010; Lupo et al., 2021; Angue Zogo et al., 2022). In western Cameroon, Shum Laka revealed a sequence consisting of an evolving LSA lithic industry and the gradual pottery introduction from the 5th to the 2nd millennium BCE (Lavachery, 2001).

Due to its coherent stratigraphy and abundant lithic material, Mukila (*MUK2018* and *MUK1952*) provides unique new insights while enlarging the body of archaeological sites in Central Africa. The site presents lithics that span the Late Pleistocene and Holocene (LSA to Iron Age) and asserts lithic production until the turn of time. Lithic production at Mukila may have existed until pottery's introduction in the Late Iron Age (14th to 17th century CE). However, modern disturbances of the upper 40 cm make it challenging to confirm that.

While the excavations at Mukila revealed considerably young lithics dating to the last millennia BCE, they failed to uncover contemporary ceramics. The closest site to Mukila with Early Iron Age pottery is Gombe, about 200 km west (Fig. 1A; de Maret, 1982: 77–79; 1986: 127–128; 1990: 454 Fig. 4; de Maret and Stainier, 1999). With considerable disturbances preventing more detailed analyses, thermoluminescence dates on three sherds (OxTL-209a, OxTL-209c, OxTL-209d) date into the 3rd to 5th century CE (Cahen, 1981: 131). The pottery from Gombe shows some similarities to the Ngovo pottery of the Lower Congo that dates into the 4th century BCE to 1st century CE (de Maret, 1986: 130; Seidensticker, 2021: 215–216 Fig. 99: 3–5, 10–12). The Gombe pottery is also typologically similar to grog-tempered vessels from the Île des Mimosas, dating to the 4th to 7th century CE (Lv-168; de Maret, 1982: 79; Eggert, 1984: 279–280 Figs. 8–9). To the southeast of Mukila, a single radiocarbon date from the mine of Furi I, about 40 km east of Dundo in north-eastern Angola (Fig. 1A), dates into the 1st to 4th century CE (UCLA-170; Fergusson and Libby, 1963: 17). The charcoal was presumably associated with Late Stone Age lithics (Late Tshitolian) and pottery. Unfortunately, no further details on this site exist. The nearby site of Dundo airfield yielded only younger material (Clark, 1968), dating to the 7th to early 11th century CE (UCLA-716), that is partially comparable to the finds in and around Mukila. Mashita Mbanza, dating to the Late Iron Age (de Maret, 1982: 84; Pierot, 1987; Cranshof et al., 2018: 194), is the closest site east of Mukila (Fig. 1A). Further north, recent fieldwork in Kwango, Kwilu and Maï-Ndombe uncovered 140 new sites (Seidensticker et al., 2018; Matonda et al., 2019, 2021;

Coutros et al., 2022, 2023). At multiple sites, pottery reminiscent of Early Iron Age styles further west was identified (Matonda et al., 2019: 21–23; 2021: 27). The pottery inventory from Mukila only shows characteristics linking it to the Late Iron Age Kongo Type B of the Lower Congo and the contemporaneous pottery from Dundo Airfield in north-eastern Angola. There are no indicators for the Mukila ceramic inventory to date to the Early Iron Age. Though ceramics have existed west and north of this region since the 1st millennium BCE, they occurred at the site only in the later first millennium CE.

Mukila depicts a unique situation within the context of changing lifestyles during the 1st millennium BCE in Central Africa. While the site shows lithic production until the turn of time, there are no indicators for contemporaneous ceramics. The regional overview shows a segmented and mosaic-like situation in which pottery finds appear in the archaeological records of sites further to the west and north. Only future, extended fieldwork at Mukila and its surroundings can verify how representative this lack of Early Iron Age pottery is, as such sites may be located more towards the river valley.

In the future, we must consider separate pathways for the distribution of individual cultural aspects, entailing only partial adaptation or even rejection of material goods or cultural practices. Subsistence practices and material culture must not be assumed to have spread as a single culture complex (Miller, 1969; Robertson and Bradley, 2000; Eggert, 2016), and different site types must be explored to clarify the transition from the Late Stone Age to the Early Iron Age on a local level before aiming at generalisations.

## 6. Conclusions

The combination of a reassessment of museum collections and the analysis of recently excavated material at the site of Mukila provides an archaeological and anthracological sequence spanning the late Pleistocene and the entire Holocene. The lack of clearly differentiable sediment layers and potential vertical admixture led to a multi-disciplinary approach incorporating charcoal diversity to provide meaningful stratigraphic units. Distribution of lithic and pottery finds and radiometric data respect the zones identified within the charcoal diversity. The sequence at Mukila shows several phases of occupation, supported by multiple radiocarbon dates. This does not support the hypothesis that considerable disturbances of open-air sites dating into the late Pleistocene and Holocene, as documented at Gombe, are a regionally recurrent phenomenon. Our analysis rebuts any generalisations concerning disturbances at open-air sites and urges a thorough re-evaluation of such sites through a multi-disciplinary approach.

Additionally, our research indicates lithic tool production and use up into the 1st millennium BCE, without any signs of pottery production or use during that time. Thus, younger lithic layers at Mukila represent an intriguing insight into the latest Late Stone Age, a considerably under-researched topic in Central African archaeology. It is necessary to evaluate the "end" of lithic use and production in the region to plausibly explain the environment into which (early) pottery was introduced. Open-air sites like Mukila can certainly support future research into the latest Late Stone Age.

## Funding

K.J. was supported by the Fonds Wetenschappelijk Onderzoek (FWO) PhD scholarships 1170019N & 1170021N; D.S. and W.H. were supported by the BantuFirst project, funded by the European Research Council (ERC) Consolidator Grant 724275 to K.B. D.S. is currently supported by the FWO Postdoctoral scholarship (1287922N). W.H. is presently supported by the Belgian Science Policy Office (Belspo) through the research profile FED-tWIN2019-prf-075 (CongoFORCE). Fieldwork by K.J. and D.S. at Mukila in 2018 was funded by the ERC BantuFirst project. Radiocarbon dates included in this study were supported by the ERC BantuFirst project (K.B.) and the FWO Postdoctoral scholarship (D.S.).

## Author's contributions

K.J. and D.S. designed this research and conducted fieldwork in 2018. K.J. studied all lithic inventories, and D.S. analysed all ceramic finds. W.H. studied the charcoal assemblage, F.M. conducted grain-size analyses, and E.C. facilitated the archival and collection research at RMCA.K.J., D.S., W.H., F.M. and E.C. wrote the manuscript. All co-authors commented on and approved the manuscript.

## Declaration of competing interest

The authors declare that they have no known competing financial interests or personal relationships that could have appeared to influence the work reported in this paper.

## Data availability

All data and R scripts to reproduce the analyses generated during this research are available at https://doi.org/10.5281/zenodo.11575832

## Acknowledgements

We thank the Congolese authorities for making our research possible, especially the former director of the Institut des Musées Nationaux du Congo (IMNC) in Kinshasa, Prof. Bakwa-Lufu, and his staff. We thank Jeanine Yogolelo and Clement Mambu (both IMNC) for their support during the fieldwork in 2018. We are particularly grateful to Clovis Mbuya Makstila, the prefect of the Lycée Kilenge at Mukila, for permitting us to excavate and to the entire community of Mukila for their hospitality. Special thanks go to the local excavation assistants Jean-Marie, Marc and Henock for supporting the excavation. The detailed record-keeping of the Royal Museum for Central Africa's staff aided immensely in analysing the museum collections due to the reliable traceability of the object's locations.

## Appendix A. Supplementary data

Supplementary data to this article can be found online at https://doi.org/10.1016/j.quascirev.2024.108752.

## References

Ambrose, S.H., 1998. Chronology of the later stone age and Food production in east Africa. J. Archaeol. Sci. 25, 377–392.
Angue Zogo, M.-J., de Saulieu, G., Mesfin, I., Oslisly, R., 2022. La grotte de Youmbidi, Ogooué-Lolo, Gabon : un nouveau terrain pour l'étude pluridisciplinaire du Later Stone Age en Afrique centrale atlantique. Nyame Akuma 20–37.
Bequaert, M., 1952. Fouilles a Dinga (Congo belge). In: Actes Du Congrès Panafricain de Préhistoire, pp. 347–353.
Bequaert, M., 1953. La Préhistoire du Congo Belge et ses relations avec la Préhistoire Africaine Sud-Saharienne à l'Holocène.
Bequaert, M., 1955. Fouilles à Dinga (Congo Belge). In: Balout, L. (Ed.), Actes du IIIème Congrès Panafricain de Préhistoire et de l'étude du Quaternaire. Edita, Casablanca, pp. 347–353.
Bequaert, M., 1956a. De prehistorie en protohistorie van Belgisch-Congo en van Ruanda-Urundi als een episode in de culturele opgang van de autochtonen in dit gebied, pp. 25–36.
Bequaert, M., 1956b. Préhistoire au Congo-Belge: Fouilles de 1950-1952. In: Ruggles Gates, R. (Ed.), Actes du IVe congrès international des sciences anthropologiques et ethnologiques (Vienne, 1-8 septembre 1952). Adolf Holzhausen, Wien, pp. 30–35.
Bequaert, M., 1956c. Recherches archéologiques au Kwango en 1952. In: Actes du 4ème Congrès International des Sciences Préhistoriques, pp. 29–45. Madrid. Zaragoza, Madrid.
Bevan, A., Crema, E., 2022. Rcarbon: calibration and analysis of radiocarbon dates. R-Package v1.5.9. https://cran.r-project.org/web/packages/rcarbon/index.html.
Borcard, D., Gillet, F., Legendre, P., 2011. Numerical Ecology with R, Use R. Springer, New York.
Cahen, D., 1976. Nouvelles fouilles à la point de la Gombe (ex-point de Kalina), Kinshasa, Zaïre. L'Anthropologie 80, 573–602.

Cahen, D., 1978. Vers une révision de la nomenclature des industries préhistoriques de l'Afrique centrale. L'Anthropologie 82, 5–36.
Cahen, D., 1981. Contribution à la chronologie de 1 'âge du fer dans la région de Kinshasa (Zaïre). In: Roubet, C., Senghor, L.S. (Eds.), Préhistoire Africaine, Recherche Sur Les Grandes Civilisations Synthèse. Éd. A.D.P.F, Paris, pp. 127–137.
Cahen, D., Keeley, L.H., 1980. Not less than two, not more than three. World Archaeol. 12, 166–180. https://doi.org/10.1080/00438243.1980.9979790.
Cahen, D., Lepersonne, J., 1952. Équivalence entre le Système du Kalahari du Congo belge et les Kalahari beds d'Afrique australe. Mémoires de la Société belge de géologie, de paléontologie et d'hydrologie. Série in-8° 4, 1–64.
Cahen, D., Moeyersons, J., 1977. Subsurface movements of stone artefacts and their implications for the prehistory of Central Africa. Nature 266, 812–815. https://doi.org/10.1038/266812a0.
Cahen, D., Moeyersons, J., Mook, W.G., 1983. Radiocarbon dates from Gombe point (Kinshasa, Zaïre) and their implications. In: Mook, W.G., Waterbolk, H.T. (Eds.), PACT 8: Proceedings of the First International Symposium 14C and Archaeology, Groupe Pact Editions. Council of Europe, Strassbourg, pp. 441–452.
Cahen, D., Mortelmans, G., 1973. Un site Tchitolien sur le plateau des bateke (République du Zaire).
Clark, J.D., 1968. Further Paleo-anthropological studies in northern Lunda. Publicações culturais da Companhia de Diamantes de Angola. Museu do Dundo, Lissabon.
Clark, J.D., 1971. Problems of archaeological nomenclature and definition in the Congo basin. S. Afr. Archaeol. Bull. 26, 67–78.
Clarkson, C., Jacobs, Z., Marwick, B., Fullagar, R., Wallis, L., Smith, M., Roberts, R.G., Hayes, E., Lowe, K., Carah, X., Florin, S.A., McNeil, J., Cox, D., Arnold, L.J., Hua, Q., Huntley, J., Brand, H.E.A., Manne, T., Fairbairn, A., Shulmeister, J., Lyle, L., Salinas, M., Page, M., Connell, K., Park, G., Norman, K., Murphy, T., Pardoe, C., 2017. Human occupation of northern Australia by 65,000 years ago. Nature 547, 306–310. https://doi.org/10.1038/nature22968.
Clist, B., Nikis, N., de Maret, P., 2018. Séquence chrono-culturelle de la poterie kongo (13e-19e siècles). In: Clist, B., de Maret, P., Bostoen, K. (Eds.), Une archéologie des provinces septentrionales du royaume Kongo. Archaeopress, Oxford, pp. 243–279.
Cornelissen, E., 1996. Shum Laka (Cameroon): late Pleistocene and early Holocene deposits. In: Pwiti, G., Soper, R. (Eds.), Aspects of African Archaeology. Harare: Univ. Of Zimbabwe Publ (Papers from the Congress of the Pan-African Association for Prehistory and Related Studies, vol. 10. Univ. of Zimbabwe Publ., Harare, pp. 257–263.
Cornelissen, E., 2002. Human Responses to changing environments in central Africa between 40,000 and 12. 000 B.P. Journal of World Prehistory 39.
Cornelissen, E., 2003. On Microlithic quartz industries at the end of the Pleistocene in central Africa: the Evidence from Shum Laka (NW Cameroon). Afr. Archaeol. Rev. 20, 1–24.
Cornelissen, E., 2023. Challenges and Opportunities during the Last Glacial Maximum at the Forest Margins in Central Africa. Défis et opportunités aux abords de la forêt tropicale à la fin du Pléistocène en Afrique centrale. In: Lesur, J., Cauliez, J., Khalidi, L., Bruxelles, L., Crevecoeur, I., Pleurdeau, D., Tribolo, C., Bon, F. (Eds.), Du Big Dry à l'Holocène En Afrique de l'Est et Au-Delà. From the Big Dry to the Holocene in Eastern Africa and beyond. Actes de La Séance de La Société Préhistorique Française de Toulouse (Septembre 2019), Séances de La Société Préhistorique Française. Société préhistorique française, Paris, pp. 143–158.
Cornelissen, E., Livingstone Smith, A., 2015. De archeologie can Congo in kaart gebracht. De geschiedenis van 130 jaar veldwerk. M&L Monumenten. Landschappen en Archeologie 34, 4–27.
Coutros, P.R., Matonda Sakala, I., Mabuaka Duki, A., Nkanu Tsatsa, I., Bostoen, K., 2022. The BantuFirst project: 2021 Fieldwork report on the Kwilu-Kasaï-Kamtsha-Loange River reconnaissance mission. Nyame Akuma 97, 14–21.
Coutros, P.R., Matonda Sakala, I., Mabuaka Duki, A., Nkanu Tsatsa, I., Bostoen, K., 2023. The BantuFirst project: 2022 fieldwork report on the Kwilu-Kasai river reconnaissance and Mashita Mbanza excavations (Democratic Republic of the Congo). Nyame Akuma 99, 29–34.
Cranshof, E., Nikis, N., de Maret, P., 2018. Ceramics decorated with Woven Motifs: an archaeological kongo Kingdom identifier? In: Bostoen, K.A.G., Brinkman, I. (Eds.), The Kongo Kingdom: the Origins, Dynamics and Cosmopolitan Culture of an African Polity. Cambridge University Press, Cambridge, pp. 165–196.
Creppe, N., 1935. Note sur la découverte de vestiges d'industrie lithique à Banningville (Congo Belge). Annales de la Société Géologique de Belgique, Publications relatives au Congo Belge, Annexe T LIX, 45–54.
Cziesla, E., 1990. On refitting of stone artefacts. In: Cziesla, E., Eickhoff, S., Arts, N., Winter, D. (Eds.), The Big Puzzle: International Symposium on Refitting Stone Artefacts, Monrepos, 1987, Studies in Modern Archaeology. Presented at the International Symposium on Refitting Stone Artefacts. Holos, Bonn, pp. 9–44.
de Bayle des Hermens, R., Lanfranchi, R., 1978. L'abri Tshitolien de Ntadi-Yomba (République du Congo). L'Anthropologie 82, 539.
de Maret, P., 1982. The Iron age in the west and south. In: van Noten, F.L. (Ed.), The Archaeology of Central Africa. Akademische Druck- U. Verlagsanstalt. Graz, pp. 77–96.
de Maret, P., 1986. The Ngovo Group: an industry with polished stone tools and pottery in Lower Zaïre. Afr. Archaeol. Rev. 4, 103–133.
de Maret, P., 1990. Le Néolithique et l'âge du fer ancien dans le Sud-Quest de l'Afrique Central. In: Lanfranchi, R., Schwartz, D. (Eds.), Paysages Quaternaires de l'Afrique Centrale Atlantique, Collection Didactiques. ORSTOM, Paris, pp. 447–457.
de Maret, P., Stainier, P., 1999. Excavations in the upper levels at Gombe and the early ceramic industries in the Kinshasa area (Zaïre). In: Smolla, G., Herrmann, F.R., Schmidt, I., Verse, F. (Eds.), Festschrift Für Günter Smolla, Materialien Zur Vor- Und Frühgeschichte von Hessen. Landesamt für Denkmalpflege Hessen, Wiesbaden, pp. 477–486.
De Ploey, J., Lepersonne, J., Stoops, G., 1968. Sédimentologie et origine des sables de la série des sables ocre et de la série des grès polymorphes (système du Kalahari) au Congo occidental, Annalen/Koninklijk Museum voor Midden-Afrika, Tervuren. Sci. Geol. 61. Tervuren.
Discamps, E., Thomas, M., Dancette, C., Gravina, B., Plutniak, S., Royer, A., Angelin, A., Bachellerie, F., Beauval, C., Bordes, J.-G., Deschamps, M., Langlais, M., Laroulandie, V., Mallye, J.-B., Michel, A., Perrin, T., Rendu, W., 2023. Breaking free from field layers: the interest of post-excavation stratigraphies (PES) for producing reliable archaeological Interpretations and increasing chronological resolution. J Paleo Arch 6, 29. https://doi.org/10.1007/s41982-023-00155-x.
Dupré, M.-C., Pinçon, B., 1997. Métallurgie et politique en Afrique centrale: Deux mille ans de vestiges sur les plateaux batéké. Gabon, Congo, Zaïre. Karthala, Paris.
Eggert, M.K.H., 1984. Imbonga und Lingonda: Zur frühesten Besiedlung des zentralafrikanischen Regenwaldes. Beiträge zur Allgemeinen und Vergleichenden Archäologie 6, 247–288.
Eggert, M.K.H., 2016. Geneticizing Bantu: historical insight or historical Trilemma? Medieval Worlds 4, 79–90. https://doi.org/10.1553/medievalworlds_no4_2016s79.
Eggert, M.K.H., 2019. Agriculture, horticulture, vegeculture, arboriculture and related problems in the Central African rainforest: old questions revisited. In: Eichhorn, B., Höhn, A. (Eds.), Trees, Grasses and Crops: People and Plants in Sub-saharan Africa and beyond, Frankfurter Archäologische Schriften. Verlag Dr. Rudolf Habelt GmbH, Bonn, pp. 73–79.
Eggert, M.K.H., Höhn, A., Kahlheber, S., Meister, C., Neumann, K., Schweizer, A., 2006. Pits, Graves and grains: archaeological and Archaeobotanical research in southern Cameroon. J. Afr. Archaeol. 4, 273–298.
Emphoux, J.-P., 1970. La grotte de Bitorri au Congo-Brazzaville. Cah. ORSTOM - Ser. Sci. Hum. 7, 3–20.
Fergusson, G.J., Libby, W.F., 1963. UCLA radiocarbon dates II. Radiocarbon 5, 1–22. https://doi.org/10.1017/S0033822200036742.
Fiedler, L., Preuß, J., 1985. Stone tools from the Inner Zaire Basin (Région de l'Equateur, Zaire). Afr. Archaeol. Rev. 3, 179–187.
Floss, H., 2012. Grundbegriffe der Artefaktmorphologie und der Bruchmechanik. In: Floss, H. (Ed.), Steinartefakte: vom Altpaläolithikum bis in die Neuzeit, Tübingen publications in prehistory. Kerns Verl, Tübingen, pp. 117–132.
Haddon, I.G., McCarthy, T.S., 2005. The Mesozoic-Cenozoic interior sag basins of central Africa: the late-Cretaceous-Cenozoic Kalahari and Okavango basins. J. Afr. Earth Sci. 43, 316–333.
Hahn, J., 1989. Erkennen und Bestimmen von Steinartefakten : Artefaktmorphologie I: Grundbegriffe, Pseudoartefakte u. Grundproduktion. Archaeologica Venatoria, Tübingen.
Hart, T.B., Hart, J.A., Dechamps, R., Fournier, M., Ataholo, M., 1996. Changes in forest composition over the last 4000 years in the Ituri basin, Zaïre. In: van der Maesen, L.J. G., van der Burgt, X.M., van Medenbach de Rooy, J.M. (Eds.), The Biodiversity of African Plants. Proceedings of the XIVth AETFAT Congress 22–27 August 1994. Kluwer Academic Publishers, Dordrecht/Boston/London, pp. 545–563. https://doi.org/10.1007/978-94-009-0285-5_70.
Hawthorne, D., Lawson, I.T., Dargie, G.C., Bocko, Y.E., Ifo, S.A., Garcin, Y., Schefuß, E., Hiles, W., Jovani-Sancho, A.J., Tyrrell, G., Biddulph, G.E., Boom, A., Chase, B.M., Gulliver, P., Page, S.E., Roucoux, K.H., Sjögersten, S., Young, D.M., Lewis, S.L., 2023. Genesis and development of an interfluvial peatland in the central Congo basin since the late Pleistocene. Quat. Sci. Rev. 305, 107992 https://doi.org/10.1016/j.quascirev.2023.107992.
Hogg, A.G., Heaton, T.J., Hua, Q., Palmer, J.G., Turney, C.S., Southon, J., Bayliss, A., Blackwell, P.G., Boswijk, G., Bronk Ramsey, C., Pearson, C., Petchey, F., Reimer, P., Reimer, R., Wacker, L., 2020. SHCal20 southern Hemisphere calibration, 0–55,000 Years cal BP. Radiocarbon 62, 759–778. https://doi.org/10.1017/RDC.2020.59.
Hubau, W., Van den Bulcke, J., Mees, F., van Acker, J., Beeckman, H., 2012. Charcoal identification in species-rich biomes: a protocol for Central Africa optimised for the Mayumbe forest. Rev. Palaeobot. Palynol. 171, 164–178. https://doi.org/10.1016/j.revpalbo.2011.11.002.
Hubau, W., Van den Bulcke, J., van Acker, J., Beeckman, H., 2015. Charcoal-inferred Holocene fire and vegetation history linked to drought periods in the Democratic Republic of Congo. Global Change Biol. 21, 2296–2308. https://doi.org/10.1111/gcb.12844.
IAWA Committee, 1989. List of microscopic features for hardwood identification. IAWA (Int. Assoc. Wood Anat.) Bull. 10, 201–232.
Inside Wood Database, 2016. The inside wood database. URL. http://insidewood.lib.ncsu.edu/search;jsessionid=9C599A121B6B6C1A987CFD23D553BD34?0. (Accessed 9 December 2021).
Jesse, F., 2003. Rahib 80/87: Ein Wavy-Line-Fundplatz im Wadi Howar und die früheste Keramik in Nordafrika, Africa Praehistorica. Heinrich-Barth-Inst, Köln.
Juggins, S., 2012. Rioja: analysis of Quaternary Science data. R package v0.7-3. https://cran.r-project.org/package=rioja.
Jungnickel, K.V.M., in Prep. CONTACT ARCHAEOLOGY IN CENTRAL AFRICA: an Archaeological Approach to Early Interactions between Hunter-Gatherers and Sedentary Food-Producers in Western Central Africa (PhD Dissertation). Goethe-Universität, Frankfurt am Main.
Kent, S., Scholtz, N., 2003. Perspectives on the geology of an open-air middle stone age site, eastern free state, South Africa. South Afr. J. Sci. 99.
Kouyoumontzakis, G., Lanfranchi, R., Giresse, P., 1985. Les datations radiométriques de quaternaire de la République Populaire du Congo. Cahier congolais d'anthopologie et d'histoire 10, 11–31.
Lanfranchi, R., 1987. Esquisse archéologique des régions Teke. Muntu: Revue scientifique et culturelle du CICIBA 7, 73–107.

Lanfranchi, R., Pinçon, B., 1988. Résultats préliminaires des prospections archéologiques récentes sur les plateaux et collines Teke en République populaire du Congo (1984-1987). Nsi 3, 24–31.

Lanfranchi, R., Schwartz, D. (Eds.), 1990. Paysages quaternaires de l'Afrique Centrale Atlantique, Collection Didactiques. ORSTOM, Paris.

Laughlin, J.P., Kelly, R.L., 2010. Experimental analysis of the practical limits of lithic refitting. J. Archaeol. Sci. 37, 427–433. https://doi.org/10.1016/j.jas.2009.10.007.

Lavachery, P., 1990. L'age de la pierre recent au Bas-Zaire: Etude du materiel lithique des missions Bequaert 1950-1952 et de Maret 1973 (Mémoire licencié). Brussels.

Lavachery, P., 1996. Shum Laka rock shelter late Holocene deposits: from stone to metal (North Western Cameroon). In: Pwiti, G., Soper, R. (Eds.), Aspects of African Archaeology. Harare: Univ. Of Zimbabwe Publ (Papers from the Congress of the Pan-African Association for Prehistory and Related Studies, vol. 10. Univ. of Zimbabwe Publ., Harare, pp. 265–274.

Lavachery, P., 1997. De la pierre au metal. Archéologie des dépôts holocènes de l'abri du Shum Laka (Cameroun) (Dissertation). Universite libre de Bruxelles, Bruxelles.

Lavachery, P., 2001. The Holocene archaeological sequence of Shum Laka rock shelter (Grassfields, western Cameroon). Afr. Archaeol. Rev. 18, 213–247. https://doi.org/10.1023/A:1013114008855.

Lavachery, P., MacEachern, S., Bouimon, T., Mbida Mindzié, C., 2010. Komé – Kribi: Rescue archaeology along the Chad-Cameroon oil Pipeline, 1999-2004. In: Journal of African Archaeology Monograph Series. Africa Magna Verlag, Frankfurt am Main.

Lupo, K.D., Schmitt, D.N., Ndanga, J.-P., Nguerede, L.P., Amaye, G.T., Smith, A.L., Edwards, N.M., Power, R.C., Craig Young, D., Npo, F., 2021. Hunter-gatherers on the basin's edge: a preliminary look at Holocene human occupation of Nangara-Komba Shelter, Central African Republic. Azania 56, 4–33. https://doi.org/10.1080/0067270X.2020.1865636.

Matonda, I., Bigohe, S., Bostoen, K., 2019. Le projet BantuFirst: rapport sur les recherches de terrain archéologiques 2019 dans les provinces du Kwilu et de Kinshasa, République Démocratique du Congo. Nyame Akuma 92, 19–24.

Matonda, I., Bigohe, S., Mambu, C., Bostoen, K., 2021. Le projet BantuFirst: rapport sur les recherches de terrain archéologiques le long du bas Kasaï dans les provinces du Kwilu et du Mai-Ndombe (RDC). Nyame Akuma 95, 25–30.

Mayaux, P., Bartholomé, E., Massart, M., van Cutsem, C., Cabral, A., Nonguierma, A., Diallo, O., Pretorius, C., Thompson, M., Cherlet, M., Pekel, J.-F., Defourny, P., Vasconcelos, M., Di Gregorio, A., Fritz, S., de Grandi, G., Elvidge, C., Vogt, P., Belward, A.S., 2003. A Land Cover Map of Africa: Carte de l'occupation du sol de l'Afrique. EUR/European Commission. EUR-OP/European Commission, Joint Research Centre, Luxembourg.

Mercader, J., Martí, R., 2003. The middle stone age occupation of Atlantic central Africa: new Evidence from Euqatorial Guinea and Cameroon. In: Mercader, J. (Ed.), Under the Canopy. Rutgers University Press, New Brunswick and Piscataway and N.J, pp. 64–92.

Mesfin, I., Oslisly, R., Forestier, H., 2021. Technological analysis of the quartz industry of Maboué 5 – Layer 3 (Lopé National Park, Gabon): implications for the late stone age emergence in western central Africa. J. Archaeol. Sci.: Report 39, 103130. https://doi.org/10.1016/j.jasrep.2021.103130.

Miller, S.F., 1969. Contacts between the later stone age and the early Iron age in southern central Africa. Azania 4, 81–90. https://doi.org/10.1080/00672706909511508.

Miller, S.F., 1988. Patterns of environmental Utilization by late Prehistoric cultures in the southern Congo basin. In: Bower, J., Lubell, D. (Eds.), Prehistoric Cultures and Environments in the Late Quaternary of Africa. BAR International Series, Oxford, pp. 127–144.

Miller, S.F., 2001. Tshitolian. In: Peregrine, P.N., Ember, M. (Eds.), Encyclopedia of Prehistory Volume 1: Africa. Springer US, Boston, MA, pp. 278–286. https://doi.org/10.1007/978-1-4615-1193-9_24.

Moeyersons, J., 1978. The behaviour of stones and stone implements, buried in consolidating and creeping Kalahari sands. Earth Surf. Process. 3, 115–128. https://doi.org/10.1002/esp.3290030203.

Morin-Rivat, J., Fayolle, A., Gillet, J.F., Bourland, N., Gourlet-Fleury, S., Oslisly, R., Bremond, L., Bentaleb, I., Beeckman, H., Doucet, J.-L., 2014. New Evidence of human activities during the Holocene in the lowland forests of the northern Congo basin. Radiocarbon 56, 209–220.

Morrow, T.M., 1996. Lithic refitting and archaeological site formation processes. In: Odell, G.H. (Ed.), Stone Tools, Interdisciplinary Contributions to Archaeology. Springer US, Boston, MA, pp. 345–373. https://doi.org/10.1007/978-1-4899-0173-6_13.

Mortelmans, G., 1962a. Archéologie des grottes Dimba et Ngovo: Région de Thysville, Bas-Congo. In: Mortelmans, Georges, Nenquin, J. (Eds.), Actes, IVe Congrès Panafricain de Préhistoire et de l'Etude Du Quaternaire (Bd. 2): Congres Leopoldville 1959. Annalen/Koninklijk Museum Voor Midden-Afrika, Tervuren, België : Menswetenschappen = Sciences Humaines. Musée Royal de l'Afrique Centrale, Tervuren, pp. 407–425.

Mortelmans, G., 1962b. Vue d'ensemble sur la préhistoire du Congo occidental. In: Mortelmans, Georges, Nenquin, J. (Eds.), Actes, IVe Congrès Panafricain de Préhistoire et de l'Etude Du Quaternaire (Bd. 2): Congres Leopoldville 1959. Annalen/Koninklijk Museum Voor Midden-Afrika, Tervuren, België : Menswetenschappen = Sciences Humaines. Musée Royal de l'Afrique Centrale, Tervuren, pp. 129–164.

Nash, D.J., Coulson, S., Staurset, S., Ullyott, J.S., Babutsi, M., Hopkinson, L., Smith, M.P., 2013. Provenancing of silcrete raw materials indicates long-distance transport to Tsodilo Hills, Botswana, during the Middle Stone Age. J. Hum. Evol. 64, 280–288. https://doi.org/10.1016/j.jhevol.2013.01.010.

Nash, D.J., De Cort, G., Chase, B.M., Verschuren, D., Nicholson, S.E., Shanahan, T.M., Asrat, A., Lézine, A.-M., Grab, S.W., 2016. African hydroclimatic variability during the last 2000 years. Quat. Sci. Rev. 154, 1–22. https://doi.org/10.1016/j.quascirev.2016.10.012.

Nieto-Quintano, P., Mitchard, E.T.A., Odende, R., Batsa Mouwembe, M.A., Rayden, T., Ryan, C.M., 2018. The mesic savannas of the Bateke Plateau: carbon stocks and floristic composition. Biotropica 50, 868–880. https://doi.org/10.1111/btp.12606.

Oas, S.E., D'Andrea, A.C., Watson, D.J., 2015. 10,000 year history of plant use at Bosumpra Cave, Ghana. Veg. Hist. Archaeobotany 24, 635–653. https://doi.org/10.1007/s00334-015-0514-2.

Oksanen, J., Blanchet, F.G., Friendly, M., Kindt, R., Legendre, P., McGlinn, D., Minchin, P.R., O'Hara, R.B., Simpson, G.L., Solymos, P., Stevens, M.H.H., Szoecs, E., Wagner, H., 2018. Vegan: community Ecology package. R package v2 5–2. https://cran.r-project.org/web/packages/vegan/index.html.

Oslisly, R., Doutrelepont, H., Fontugne, M., Forestier, H., Giresse, P., Hatte, C., White, L., 2006. Premiers Résultats pluridisciplinaires d'une stratigraphie vieille du plus de 40000 ans du site de Maboué 5 dans la Réserve de la Lopé au Gabon. In: de Maret, P., Cornelissen, E., Ribot, I. (Eds.), Actes Du XIVème Congrès UISPP, Université de Liège, Belgique, BAR International Series, vol. 1522, pp. 189–198, 2–8 Septembre 2001.

Peel, M.C., Finlayson, B.L., McMahon, T.A., 2007. Updated World map of the Köppen-Geiger climate Classification. Hydrol. Earth Syst. Sci. 11, 1633–2007. https://doi.org/10.5194/hess-11-1633-2007.

Peyrot, B., Oslisly, R., Abdessadok, S., Fontugne, M., Christine, Hattem, White, L., 2003. Les paléoenvironnements de la fin du Pléistocène et de l'Holocène dans la réserve de la Lopé (Gabon): Approche par les indicateurs géomorphologiques, sédimentologiques, phytologiques, géochimiques et anthropogènes des milieux enregistreurs de la dépression de la Lopé. L'Anthropologie 107, 291–307.

Phillips, N., Moffat, I., Mackay, A., Jones, B.G., 2023. The sedimentary context of open-air archaeology: a case study in the western Cape's doring river valley, South Africa. Soil Systems 7, 25. https://doi.org/10.3390/soilsystems7010025.

Pierot, F., 1987. Etude ethnoarcheologique du site de Mashita Mbanza: Mémoir présenté en vue de l'obtention du-grad de licencié en Histoire de l'Art et Archéologie (Arts non Européens) (Mémoire de licencié). Universite libre de Bruxelles, Brüssel.

Pinçon, B., 1990. La métallurgie du fer sur les plateaux téké (Congo): Quelle influence sur l'évolution des paysages au cours des deux derniers millénaires? In: Lanfranchi, R., Schwartz, D. (Eds.), Paysages quaternaires de l'Afrique Centrale Atlantique, Collection Didactiques. ORSTOM, Paris, pp. 479–492.

Pinçon, B., 1991a. Archaeologie des plateau et collines Teke (Republique Populaire du Congo): De nouvelles donees. Nsi 8/9, 24–32.

Pinçon, B., 1991b. L'archéologie du royaume Teke. In: Lanfranchi, R., Clist, B. (Eds.), Aux origines de l'Afrique centrale. Centres culturels français d'Afrique centrale and Centre international des civilisations Bantu and Sépia avec le concours de UTA, Paris, pp. 243–249.

Pinçon, B., 1984. La ceramique Teke de la region de Zanaga (XIX ème - XX ème Siecle): Memoir de D. E.S. Universite Marien Ngouabi, Brazzaville.

Preuß, J., Fiedler, L., 1984. Steingeräte aus dem inneren Kongobecken und ihre geomorphologische Einbindung. Beiträge zur Allgemeinen und Vergleichenden Archäologie 6, 227–246.

Reeuwijk, L.P. van, 2002. Procedures for Soil Analysis, sixth ed. International Soil Reference and Information Centre, Wageningen. Technical paper/International Soil Reference an Information Centre.

Robertson, J.H., Bradley, R., 2000. A new paradigm: the African early Iron age without Bantu Migrations. Hist. Afr. 27, 287. https://doi.org/10.2307/3172118.

Romagnoli, F., Vaquero, M., 2019. The challenges of applying refitting analysis in the Palaeolithic archaeology of the twenty-first century: an actualised overview and future perspectives. Archaeol Anthropol Sci 11, 4387–4396. https://doi.org/10.1007/s12520-019-00888-3.

Schmidt, P., Archer, W., Porraz, G., 2021. A First Chemical Study of the Provenance of Silcretes from Diepkloof Rockshelter. South Africa.

Seidensticker, D., 2016. Archaeology and history in Iron age Settlements in the Congo basin. In: Sadr, K., Esterhuysen, A., Sievers, C. (Eds.), African Archaeology without Frontiers. Wits University Press, Johannesburg, pp. 114–126.

Seidensticker, D., 2021. Archäologische Untersuchungen zur eisenzeitlichen Besiedlungsgeschichte des nordwestlichen Kongobeckens. Tübingen University Press, Tübingen.

Seidensticker, D., Jungnickel, K., Mambu, C., Yogolelo, J., Bostoen, K., 2018. The BantuFirst project: 2018 fieldwork report from the Kinshasa, Kwango, Kwilu and Mai-Ndombe provinces of the Democratic Republic of the Congo. Nyame Akuma 90, 23–29.

Staurset, S., Coulson, S., 2014. Sub-surface movement of stone artefacts at white Paintings shelter, Tsodilo hills, Botswana: implications for the middle stone age chronology of central southern Africa. J. Hum. Evol. 75, 153–165. https://doi.org/10.1016/j.jhevol.2014.04.006.

Tafelmaier, Y., Bataille, G., Schmid, V., Taller, A., Will, M., 2022. Methods for the Analysis of Stone Artefacts: an Overview, Essentials. Springer, Fachmedien Wiesbaden, Wiesbaden. https://doi.org/10.1007/978-3-658-39091-4.

Taylor, N., 2011. The origins of hunting and gathering in the Congo basin: a Perspective of the middle stone age Lupemban industry. Before Farming 1–20. https://doi.org/10.3828/bfarm.2011.1.6.

Taylor, N., 2016. Across rainforests and Woodlands: a systematic Reappraisal of the Lupemban middle stone age in central Africa. In: Jones, S.C., Stewart, B.A. (Eds.), Africa from MIS 6-2. Springer, Netherlands, Dordrecht, pp. 273–299. https://doi.org/10.1007/978-94-017-7520-5_15.

Taylor, N., 2022. Riddles wrapped inside an enigma. Lupemban MSA technology as a rainforest adaptation: revisiting the lanceolate point. Phil. Trans. R. Soc. B 377, 20200484. https://doi.org/10.1098/rstb.2020.0484.

Thiry, M., Milnes, A., 2017. Silcretes: insights into the occurrences and formation of materials sourced for stone tool making. J. Archaeol. Sci.: Report 15, 500–513. https://doi.org/10.1016/j.jasrep.2016.08.015.

Thomas, D.S.G., Shaw, P.A., 1991. The Kalahari Environment, Nachdr. ed. Cambridge University Press, Cambridge.

van Moorsel, H., 1970. Recherches préhistoriques au pays de l'entre-fleuves Lukenie-Kasaï. Etudes Hist. Afr. I, 7–36.

van Noten, F.L., 1977. Une prospection au nord et nord-est du Zaire, vols. 9–10. Etudes d'Histoire africaine, pp. 75–77.

Vanderyst, E.P., 1950. Wombali.

Villa, P., 1982. Conjoinable pieces and site formation processes. Am. Antiq. 47, 276–290. https://doi.org/10.2307/279901.

Vleminckx, J., Morin-Rivat, J., Biwolé, A.B., Daïnou, K., Gillet, J.-F., Doucet, J.-L., Drouet, T., Hardy, O.J., 2014. Soil charcoal to assess the impacts of Past human disturbances on tropical forests. PLoS One 9, e108121. https://doi.org/10.1371/journal.pone.0108121.

Wadley, L., 1993. The Pleistocene later stone age south of the Limpopo river. J World Prehist 7, 243–296. https://doi.org/10.1007/BF00974721.

Wadley, L., 2000. The Wilton and pre-ceramic post-classic Wilton industries at Rose Cottage cave and their context in the South African sequence. S. Afr. Archaeol. Bull. 55, 90. https://doi.org/10.2307/3888959.

Wheeler, E.A., 2011. Inside Wood – a Web resource for hardwood anatomy. IAWA J. 32, 199–211. https://doi.org/10.1163/22941932-90000051.

Whittaker, J.C., 1994. Flintknapping: Making and Understanding Stone Tools, first ed. University of Texas Press, Austin.

Wright, D.K., Thompson, J.C., Schilt, F., Cohen, A.S., Choi, J.-H., Mercader, J., Nightingale, S., Miller, C.E., Mentzer, S.M., Walde, D., Welling, M., Gomani-Chindebvu, E., 2017. Approaches to middle stone age landscape archaeology in tropical Africa. J. Archaeol. Sci. 77, 64–77. https://doi.org/10.1016/j.jas.2016.01.014.